Electronic Supplementary Material (ESI) for CrystEngComm.

Taming the dynamics in a pharmaceutical by cocrystallization: investigating the impact of the coformer by solid-state NMR

Supporting Information

Patrick M.J. Szell[1], Józef R. Lewandowski[2], Helen Blade[3]*, Leslie P. Hughes[3]*, Sten O. Nilsson Lill[4]*, Steven P. Brown[1]*

*Author to whom correspondence may be addressed

[1] Department of Physics, University of Warwick, Coventry, UK, CV4 7AL. E-mail: S.P.Brown@warwick.ac.uk

[2] Department of Chemistry, University of Warwick, Coventry, UK, CV4 7AL. E-mail:

[3] Pharmaceutical Technology & Development, Operations, AstraZeneca, Macclesfield, UK. E-mail: Les.Hughes2@astrazeneca.com

[4] Early Product Development and Manufacturing, Pharmaceutical Sciences, R&D, AstraZeneca, Gothenburg, Sweden.

Table of Contents

Section I - Experimental and computational details.

T_1 fitting equations.

$$R_1 = \frac{1}{T_1} \quad \text{Eq. S1}$$

$$\tau_x = \tau_0 e^{\frac{Ea}{RT}} \quad \text{Eq. S2}$$

$$J(\omega_x, \tau_x) = \frac{2\tau_x}{1 + \omega_x^2 \tau_x^2} \quad \text{Eq. S3}$$

$$D_{CX} = -\frac{\mu_0}{4\pi} \frac{\gamma_C \gamma_X \hbar}{r_{C\cdots X}^3} \quad \text{Eq. S4}$$

$$R_1(^{13}\mathrm{C}) = C \cdot \frac{n}{15} [J(\omega_X - \omega_C) + 3J(\omega_C) + 6J(\omega_X + \omega_C)] \quad \text{Eq. S5}$$

$$C = \frac{3}{4} \cdot {D_{CX}}^2 \cdot (1 - S^2) \quad \text{Eq. S6}$$

In the equations above,[1-4] τ_x is the correlation time (s), τ_0 is the correlation time at infinite temperature (s), E_a is the activation energy (J mol^{-1}), R is the gas constant (8.3145 J K^{-1} mol^{-1}), T is the temperature (K), $J(\omega_x, \tau_x)$ is the spectral density function, ω_x is the Larmor frequency of nucleus X (rad s^{-1}), R_1 is the relaxation rate (s^{-1}), μ_0 is the vacuum permeability constant (4π x10^{-7} H m^{-1}), γ_C and γ_X are the gyromagnetic ratio of perturbing nuclei involved in the dipolar coupling (γ_{19F} = 2.52x10^8 rad T^{-1} s^{-1}; γ_{1H} = 2.68x10^8 rad T^{-1} s^{-1}; γ_{13C} = 6.73x10^7 rad T^{-1} s^{-1}), $\hbar$ is the reduced Planck constant (1.054x10^{-34} J s).

In Eq S4, $r_{X\cdots Y}$ is the internuclear X$\cdots$Y distance (C$\cdots$H = 1.09x10^{-10} m; C$\cdots$F = 1.35x10^{-10} m). In Eq S5, C is a factor given by Eq S6, n is the number of bonded hydrogen / fluorine atoms (X = H or F; n = 3 for the $^{13}CF_3$; n = 2 for $^{13}CH_2$, n = 1 for ^{13}CH). In Eq S6, S^2 is the order parameter. The order parameter (S^2) for **1**, **1b** and **1c** were calculated from a two-site jump model[5] using the torsion angles of interest from the X-ray structure (see Figure 2 of the main text and Table S37), whereas S^2 was approximated to 0.20 for **1a**, **1d** and **1e**. The value of S^2 did not affect E_a and only had a minor influence on τ_0.

Computational Details.

Table S1. Computational parameters used for the CASTEP geometry optimizations and NMR calculations.

	geometry optimization		NMR calculation	
sample	*k*-point separation ($Å^{-1}$)	cutoff energy (eV)	*k*-point separation ($Å^{-1}$)	cutoff energy (eV)
1	0.05	600	0.05	700
1a	0.1	600	0.05	700
1b	0.05	600	0.05	700
1c	0.05	600	0.05	700
1d	0.05	600	0.05	700
1e	0.05	600	0.05	600

Section II - Experimental Results.

Powder X-ray diffraction.

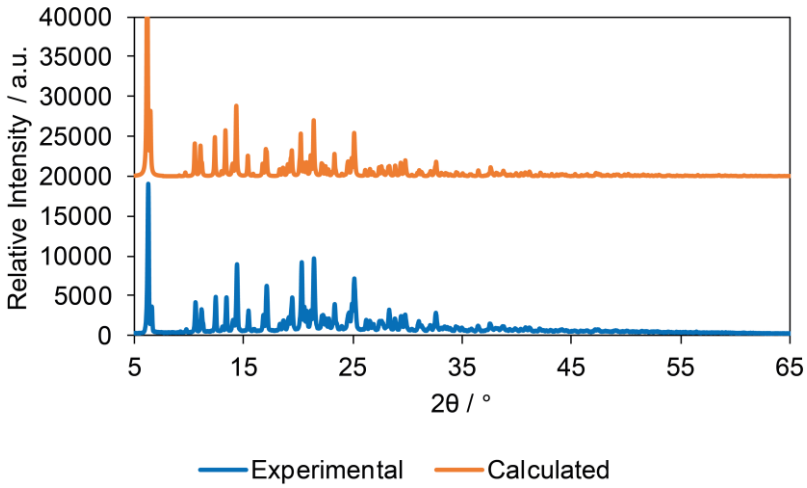

Figure S1. Experimental and calculated powder X-ray diffraction of pure **1**. The calculated pattern is for CSD structure 767883.[6]

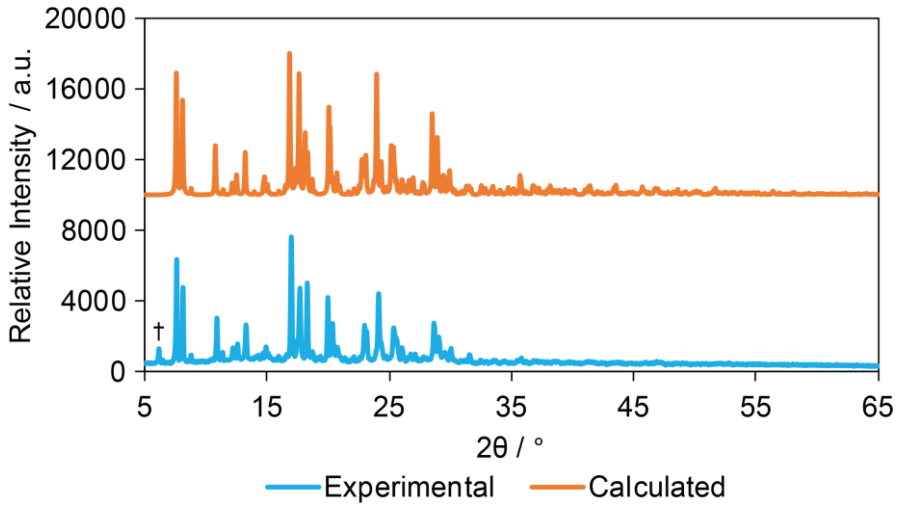

Figure S2. Experimental and calculated powder X-ray diffraction of **1a**. The dagger denotes trace amount of **1** (see Figure S1 for the PXRD of **1**). The calculated pattern of **1a** is for CSD structure 768815.[6]

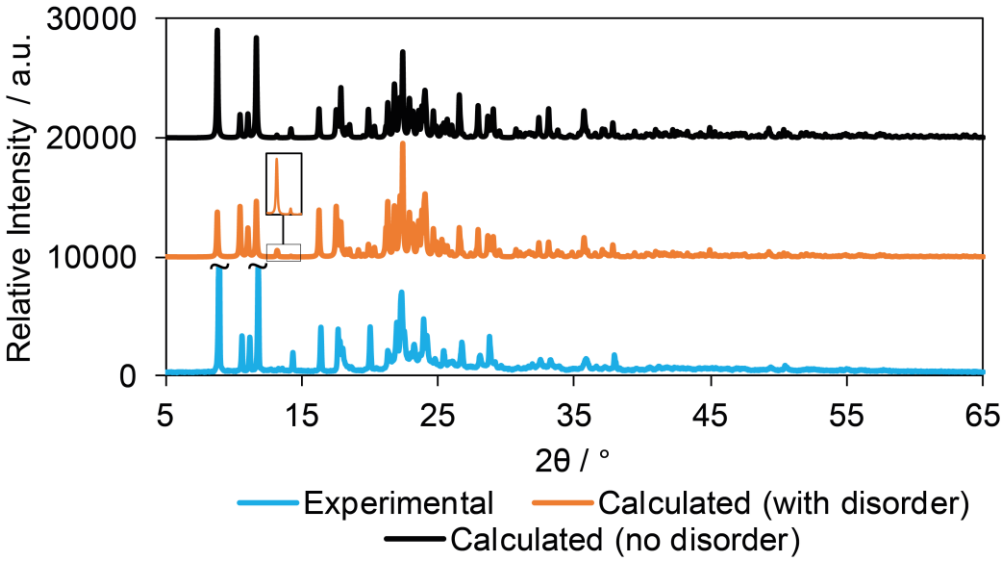

Figure S3. Experimental and calculated powder X-ray diffraction of **1b**. The calculated PXRD using the original crystal structure with disorder is shown in orange, whereas the calculated PXRD using the DFT-optimized structure without disorder is shown in black. The inset shows the low intensity of the calculated reflection at 14.1º. The calculated pattern is for CSD structure 767759.[6]

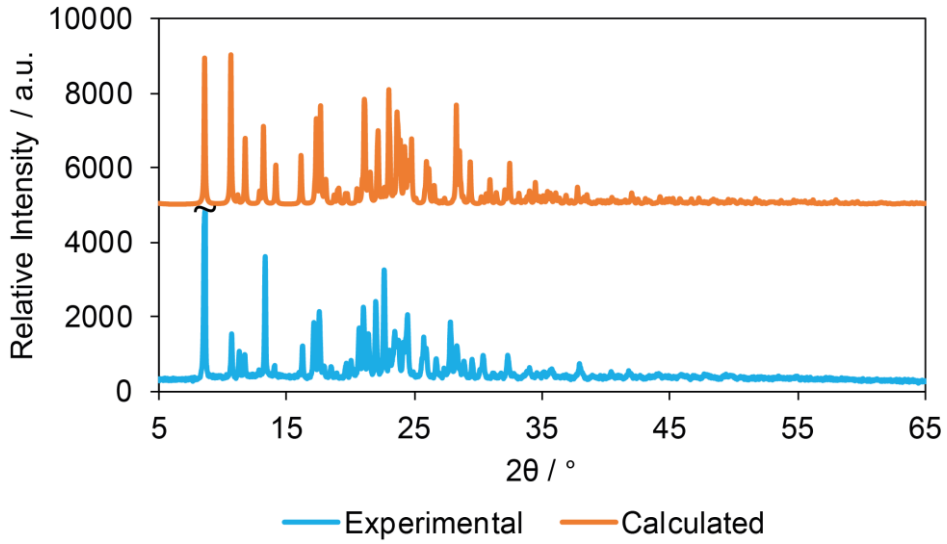

Figure S4. Experimental and calculated powder X-ray diffraction of **1c**. The calculated pattern is for CSD structure 909386.[7]

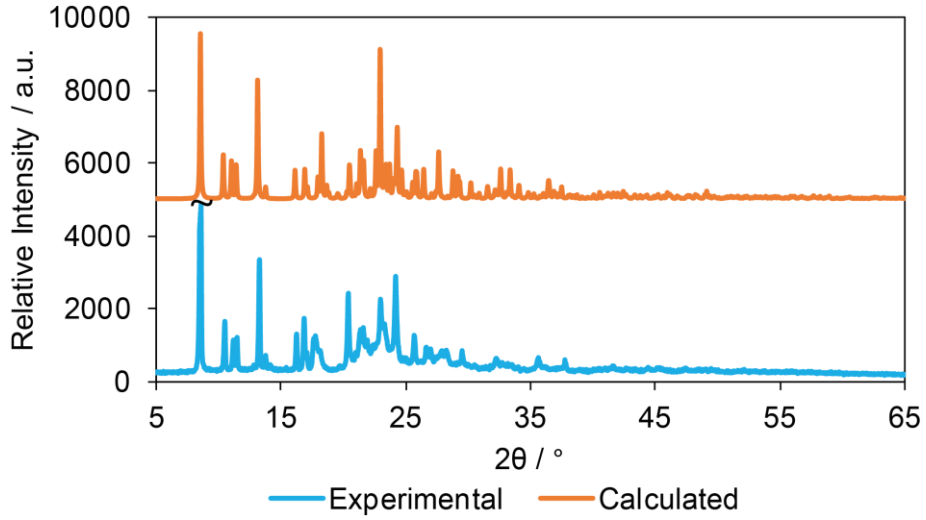

Figure S5. Experimental and calculated powder X-ray diffraction of **1d**. The calculated pattern is for CSD structure 909385.[7]

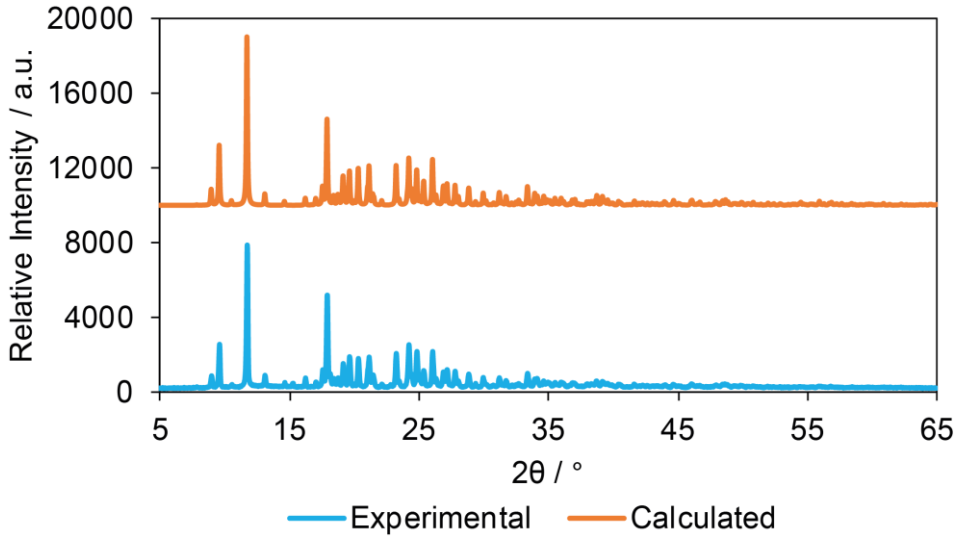

Figure S6. Experimental and calculated powder X-ray diffraction of **1e**. The calculated pattern is for CSD structure 1847168.[8]

Variable temperature ^{13}C solid-state NMR.

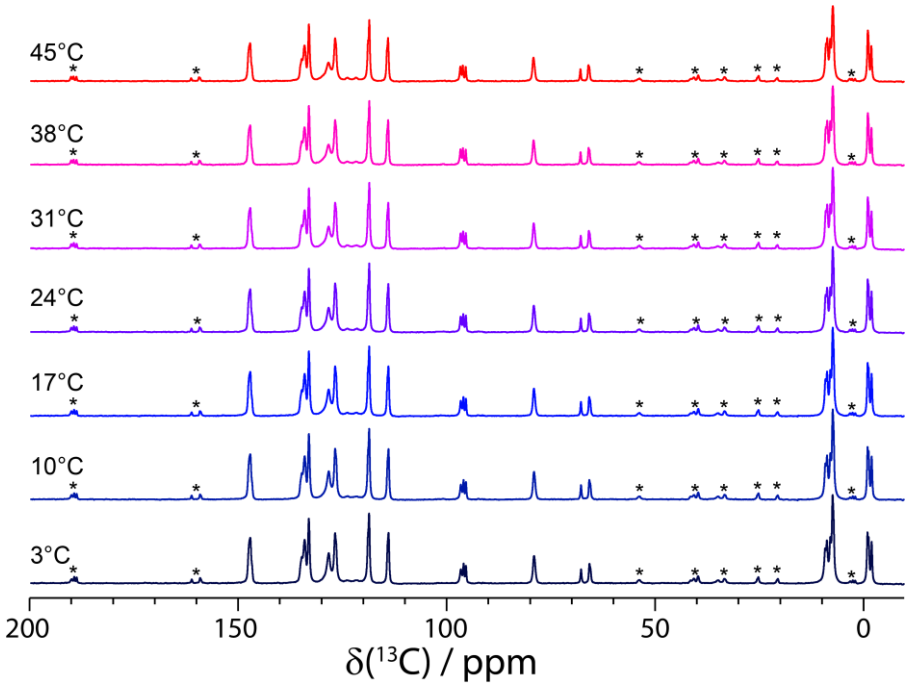

Figure S7. ^{13}C solid-state NMR spectra of **1**, pure Efavirenz, acquired at several temperatures (ν_{MAS} = 11750 Hz, $\nu_L(^{13}C)$ = 128.9 MHz, contact time = 2 ms).

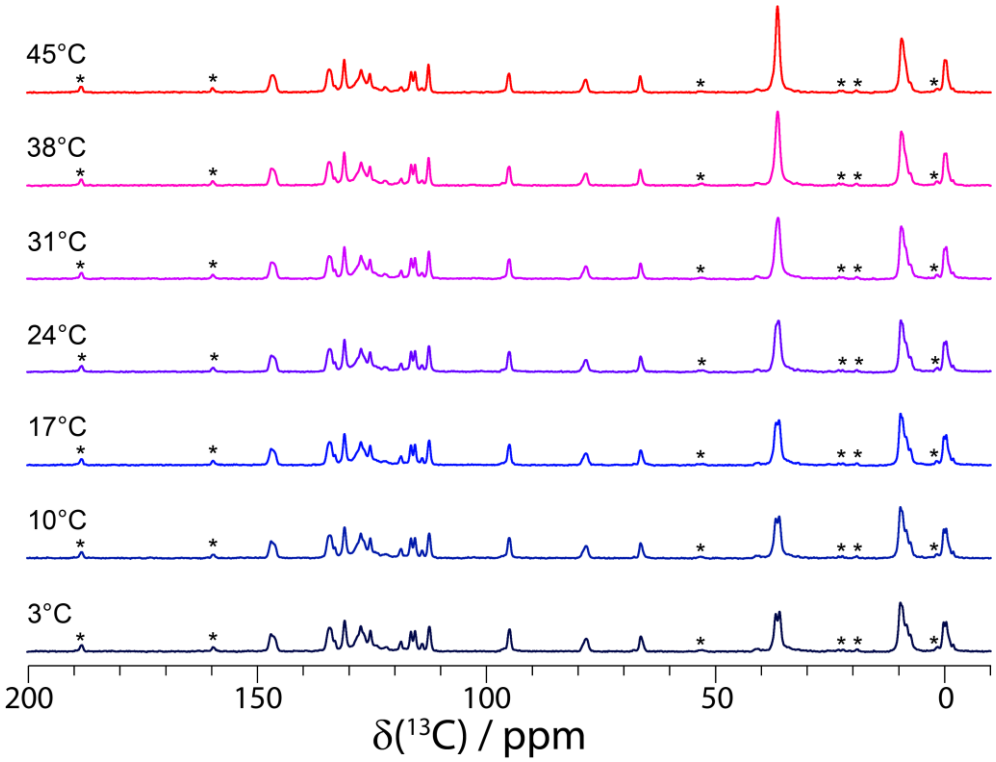

Figure S8. ^{13}C solid-state NMR spectra of **1a** acquired at several temperatures (ν_{MAS} = 11750 Hz, $\nu_L(^{13}C)$ = 128.9 MHz, contact time = 2 ms).

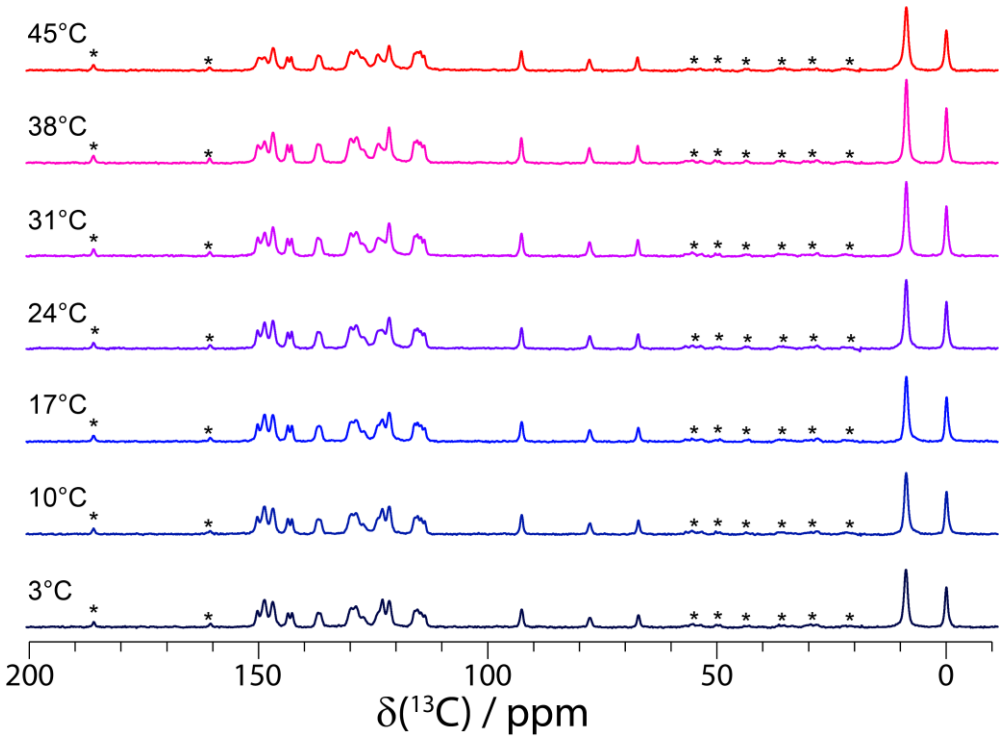

Figure S9. ^{13}C solid-state NMR spectra of **1b** acquired at several temperatures (ν_{MAS} = 11750 Hz, $\nu_L(^{13}C)$ = 128.9 MHz, contact time = 2 ms).

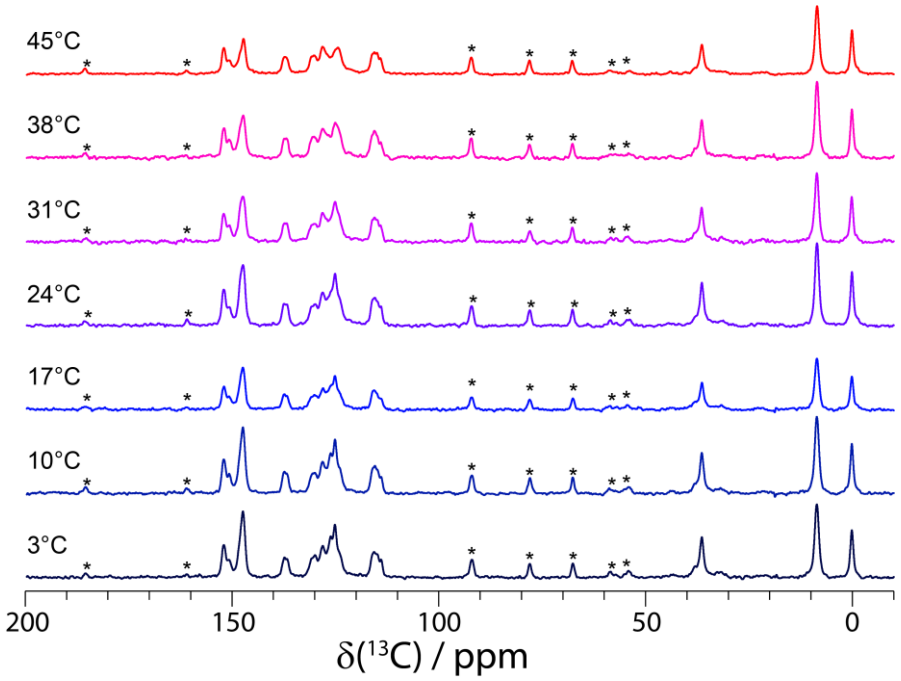

Figure S10. ^{13}C solid-state NMR spectra of **1c** acquired at several temperatures (ν_{MAS} = 11750 Hz, $\nu_L(^{13}C)$ = 128.9 MHz, contact time = 2 ms).

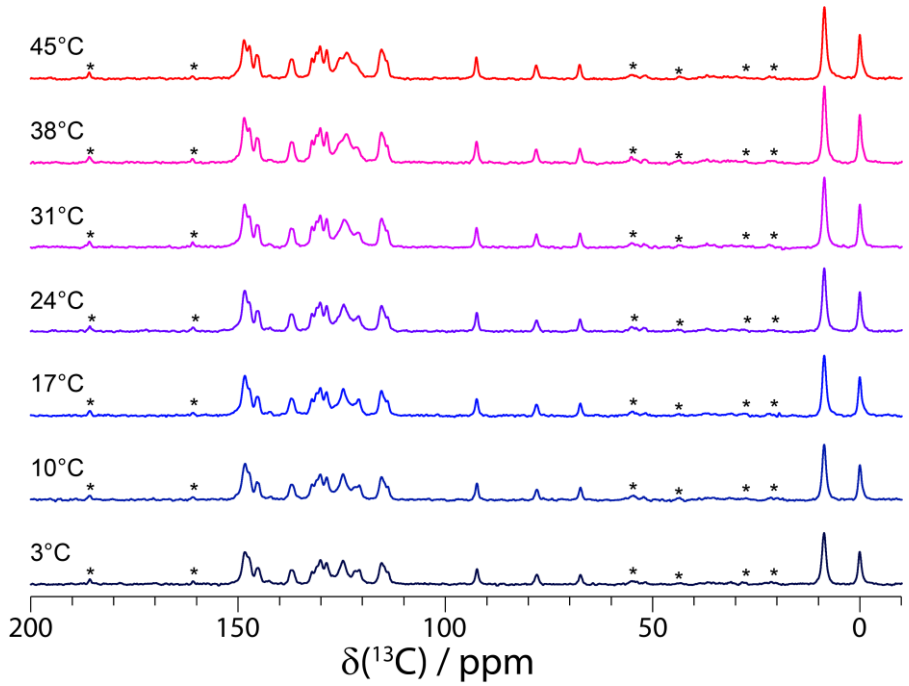

Figure S11. ^{13}C solid-state NMR spectra of **1d** acquired at several temperatures (ν_{MAS} = 11750 Hz, $\nu_L(^{13}C)$ = 128.9 MHz, contact time = 2 ms).

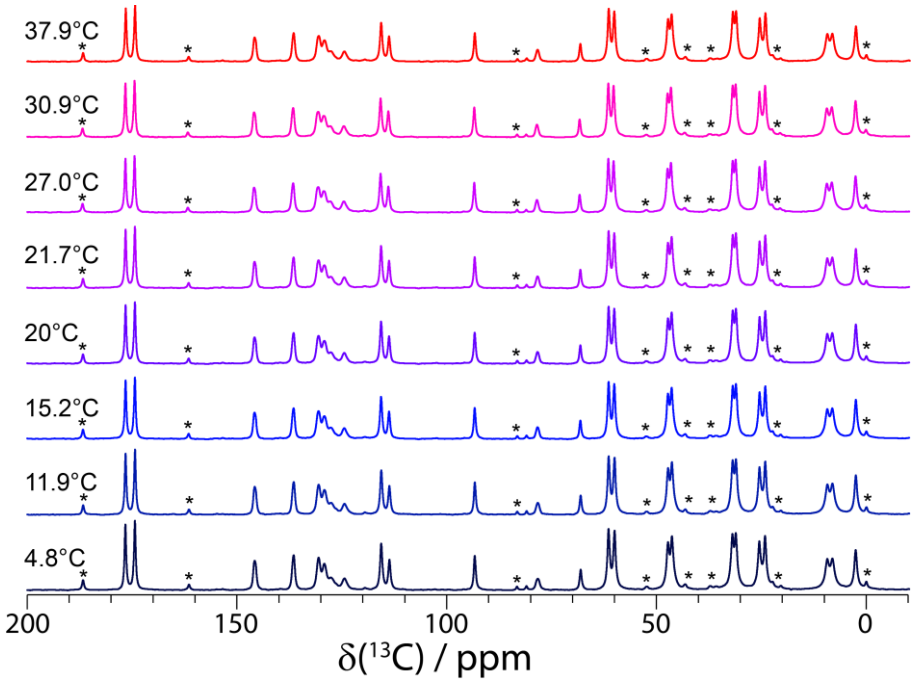

Figure S12. ^{13}C solid-state NMR spectra of **1e** acquired at several temperatures (ν_{MAS} = 11750 Hz, $\nu_L(^{13}C)$ = 128.9 MHz, contact time = 2 ms).

Variable temperature ^{19}F solid-state NMR.

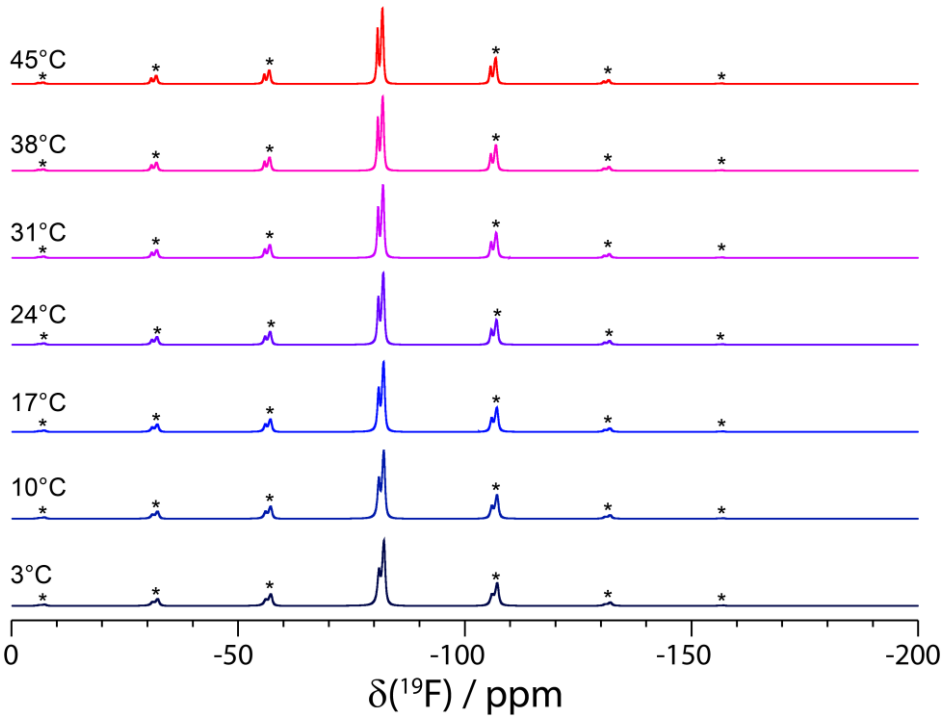

Figure S13. ^{19}F solid-state NMR spectra of **1**, pure Efavirenz, acquired at several temperatures (ν_{MAS} = 11750 Hz, $\nu_L(^{19}F)$ = 470.9 MHz).

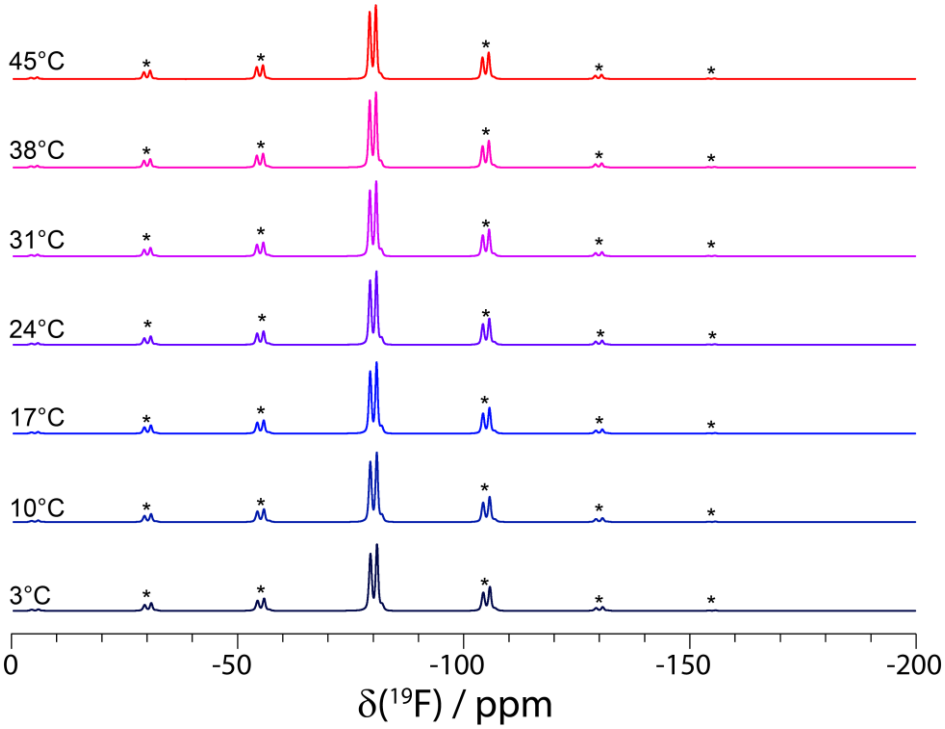

Figure S14. ^{19}F solid-state NMR spectra of **1a** acquired at several temperatures (ν_{MAS} = 11750 Hz, $\nu_L(^{19}F)$ = 470.9 MHz).

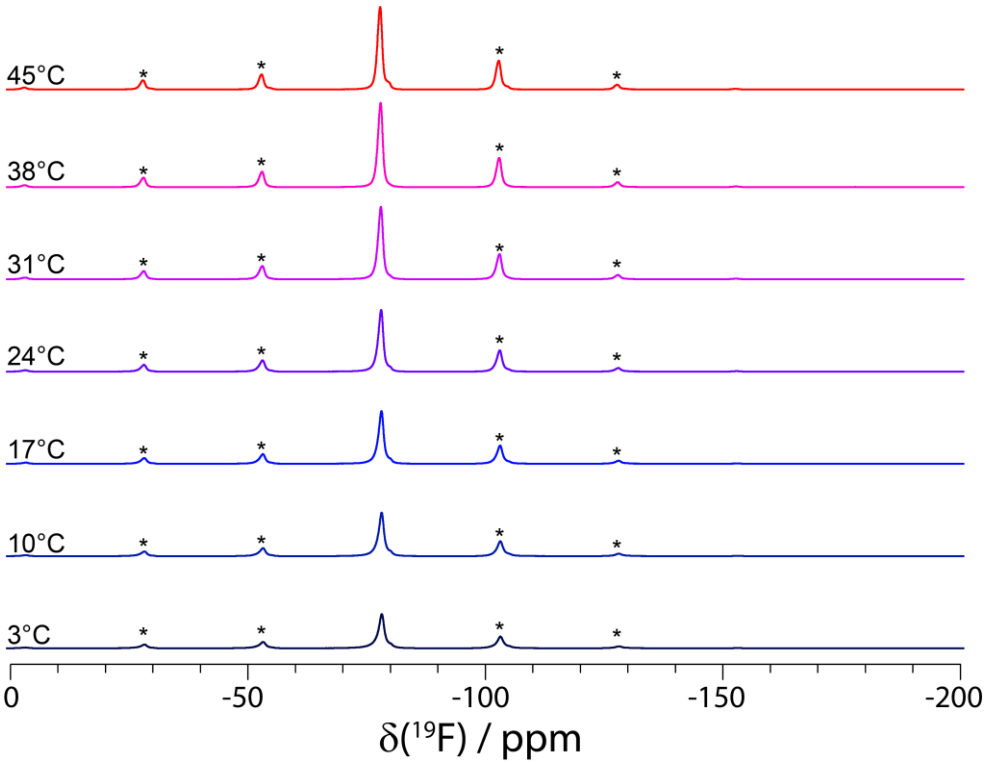

Figure S15. ^{19}F solid-state NMR spectra of **1b** acquired at several temperatures (ν_{MAS} = 11750 Hz, $\nu_L(^{19}F)$ = 470.9 MHz).

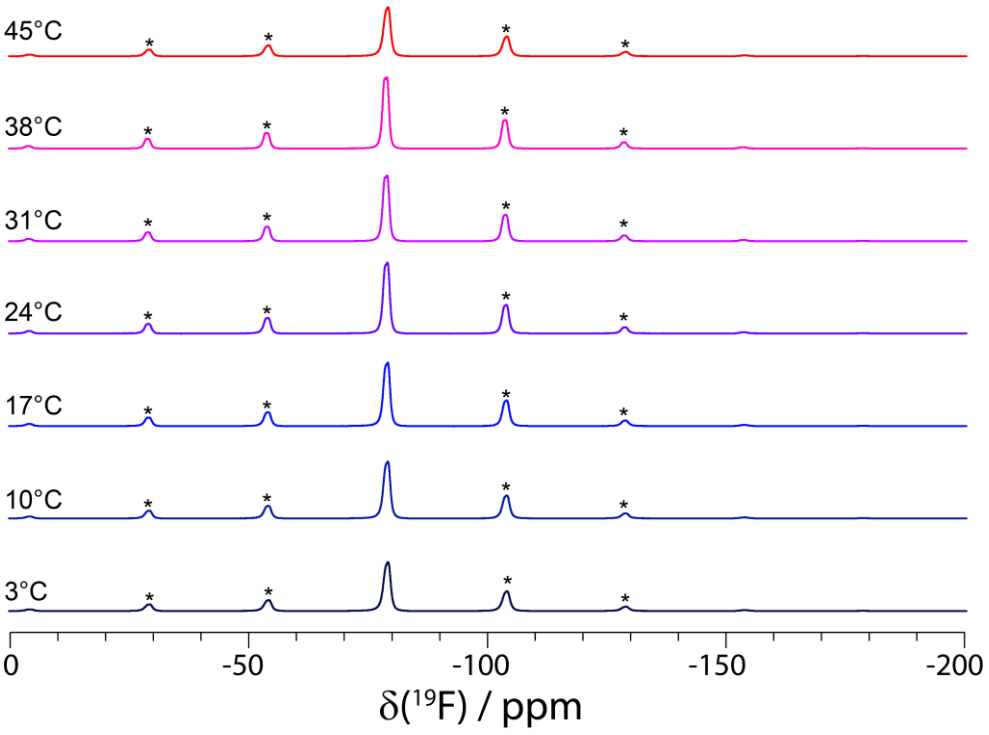

Figure S16. ^{19}F solid-state NMR spectra of **1c** acquired at several temperatures (ν_{MAS} = 11750 Hz, $\nu_L(^{19}F)$ = 470.9 MHz).

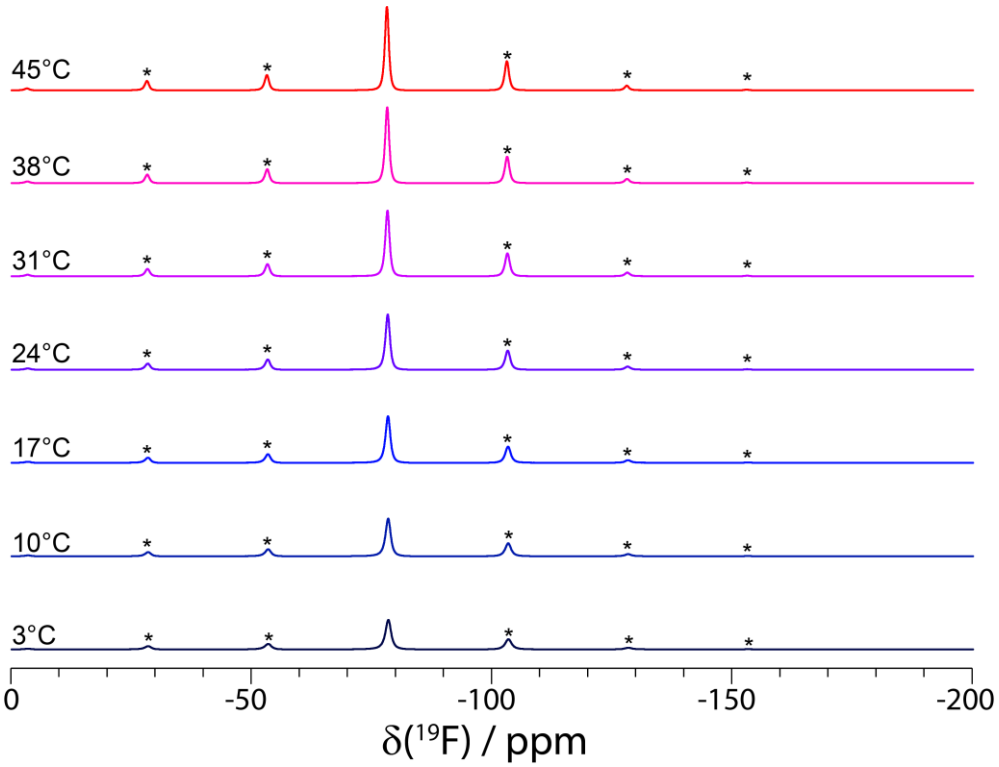

Figure S17. ^{19}F solid-state NMR spectra of **1d** acquired at several temperatures (ν_{MAS} = 11750 Hz, $\nu_L(^{19}F)$ = 470.9 MHz).

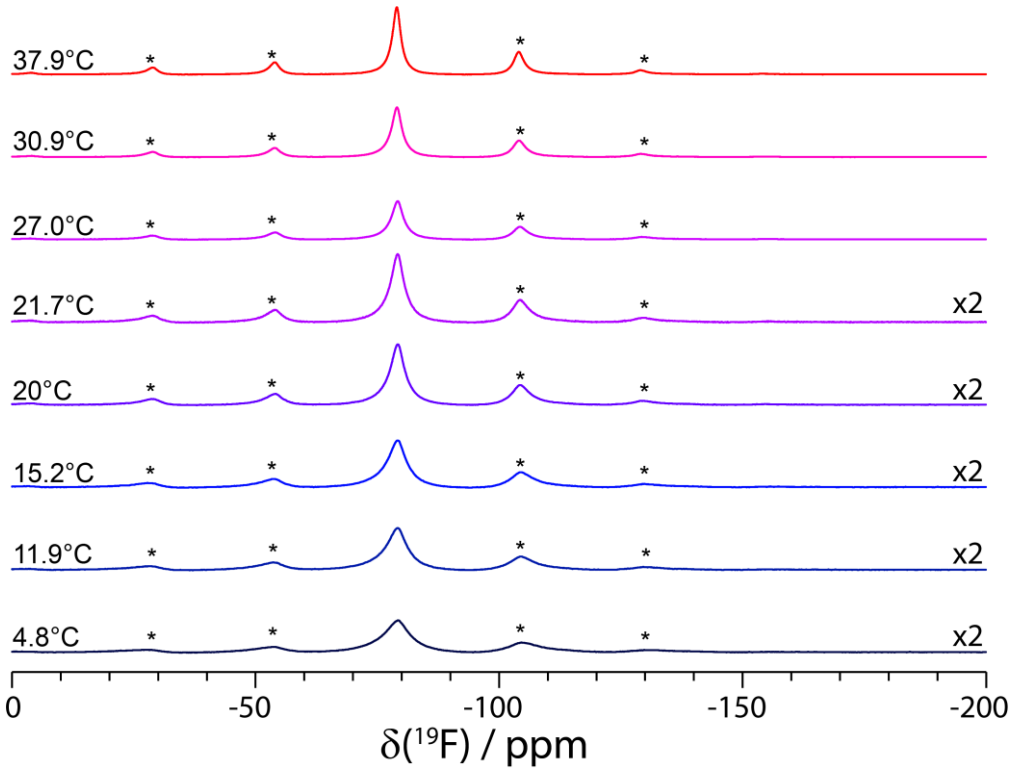

Figure S18. ^{19}F solid-state NMR spectra of **1e** acquired at several temperatures (ν_{MAS} = 11750 Hz, $\nu_L(^{19}F)$ = 470.9 MHz).

^{13}C GIPAW Simulations.

The ^{13}C solid-state NMR spectrum of **1** shows four resolved peaks for the CH_2 carbons of the cyclopropyl ring (5 to 10 ppm), which arises due to the presence of two unique CH_2 carbons on three crystallographically unique molecules (Z' = 3). The CH carbon of **1** (0 to –5 ppm) is split into two signals in a 2:1 ratio, and there are three peaks at 96 ppm, which have been assigned to the ethynyl carbon closest to the cyclopropyl group, further supporting the presence of three unique molecules of **1** in the structure (see Figure S19). In terms of **1a**, the line shape observed for the CH resonance supports the presence of two distinct molecules, as seen in the X-ray structure (Z' = 2). Unfortunately, the CH_2 resonances for the two unique cyclopropyl groups of **1a** were not resolved in the ^{13}C spectrum due to their similar chemical shifts. While two molecules are observed in the structures of **1b**, **1c**, and **1d**, a single peak was observed for both the CH_2 and CH carbons. This may be a result of the ^{13}C atoms being in similar crystallographic environments in addition to the coalescence caused by dynamics. While a single molecule is in the structure of **1e** (Z' = 1), two resonances have been observed for the CH_2 carbons of the cyclopropyl group which has been attributed to the presence of two crystallographically distinct CH_2 atoms on the cyclopropyl group.

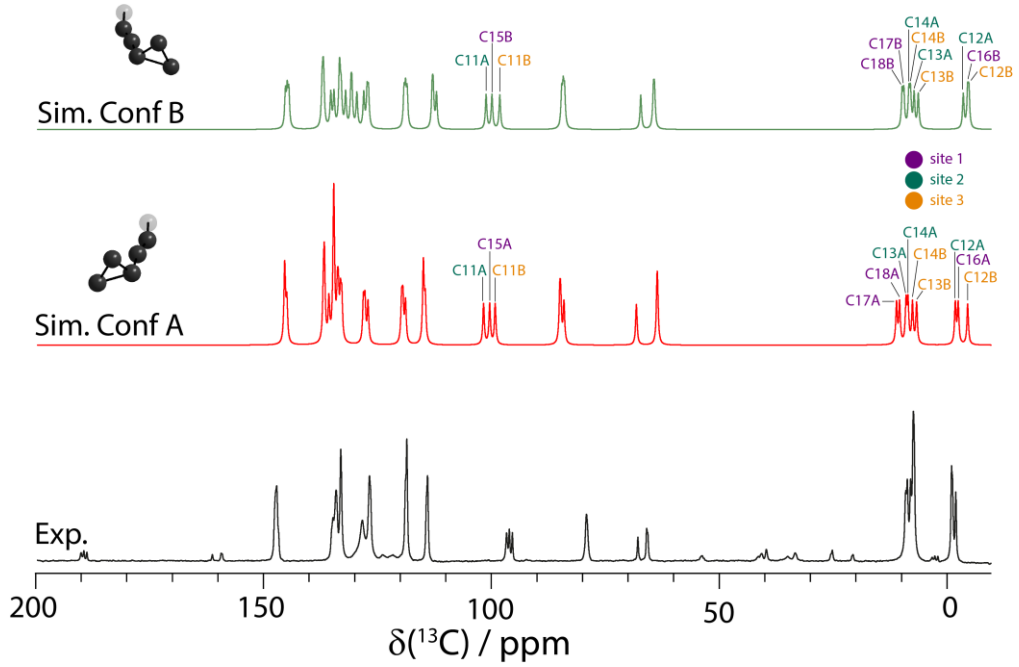

Figure S19. ^{13}C solid-state NMR spectra of **1** and the GIPAW simulated ^{13}C spectrum for both conformations of the disordered cyclopropyl group. "Conf A" denotes atom positions C16A, C17A, and C18A whereas "Conf B" denotes atom positions C16B, C17B, and C18B for the disordered cyclopropyl group.

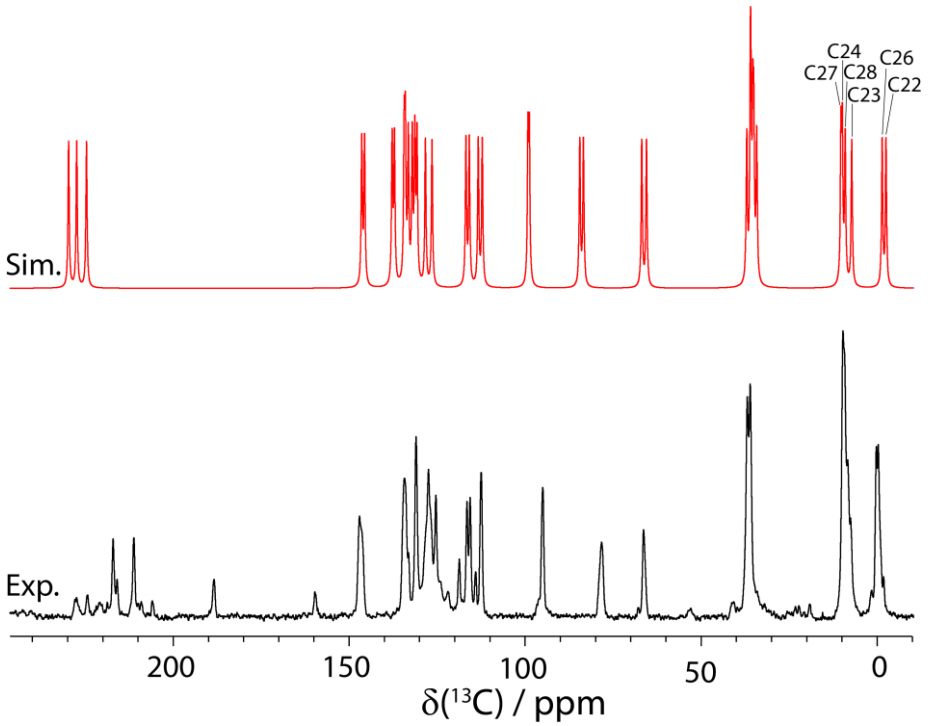

Figure S20. ^{13}C solid-state NMR spectra of **1a** and the GIPAW simulated ^{13}C spectrum for both conformations of the disordered cyclopropyl group.

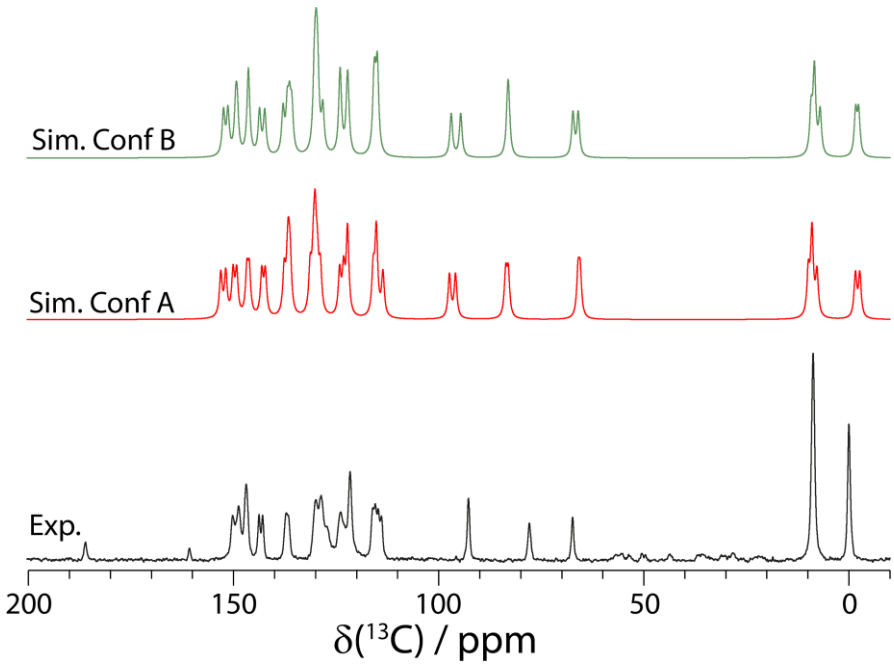

Figure S21. ^{13}C solid-state NMR spectra of **1b** and the GIPAW simulated ^{13}C spectrum for both conformations of the disordered cyclopropyl group. "Conf A" denotes atom positions C41, C51, C61, C11, C21, and C31, whereas "Conf B" denotes atom positions C41, C51, C61, C12, C22, and C32, for the disordered cyclopropyl groups.

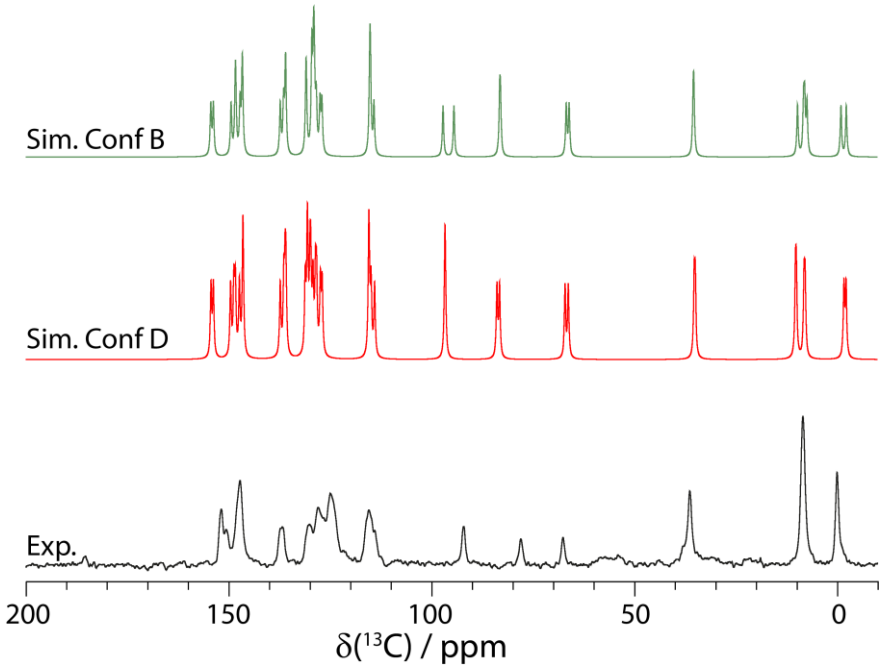

Figure S22. ^{13}C solid-state NMR spectra of **1c** and the GIPAW simulated ^{13}C spectrum for both conformations of the disordered cyclopropyl group. "Conf D" denotes atom positions C12D, C13D, and C14D whereas "Conf B" denotes atom positions C12B, C13B, and C14B, for the disordered cyclopropyl group.

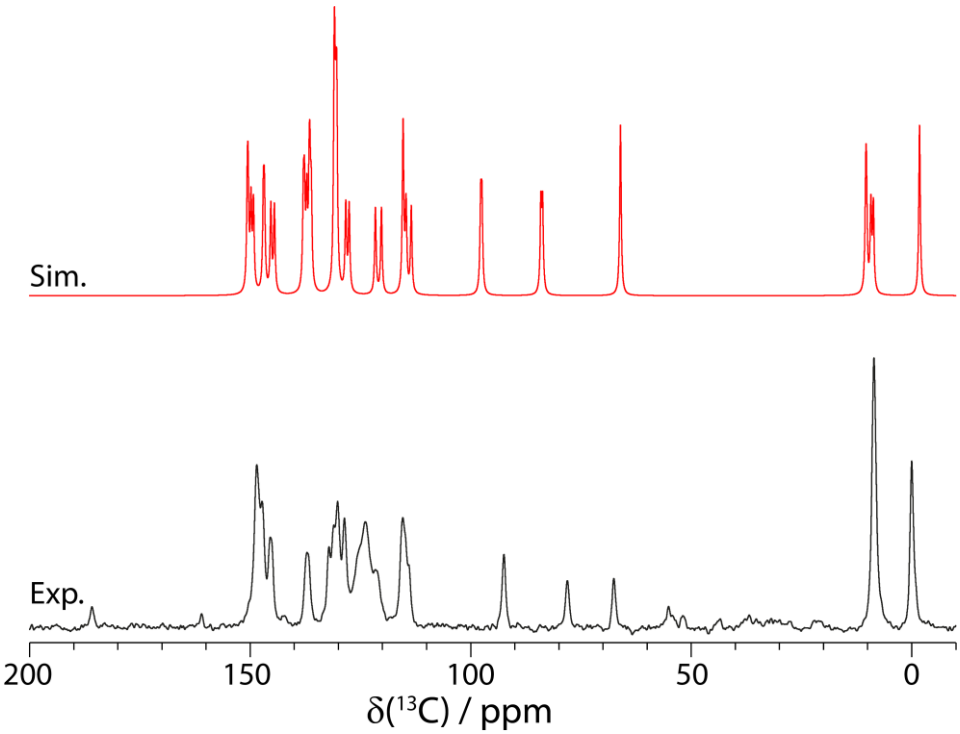

Figure S23. ^{13}C solid-state NMR spectra of **1d** and the GIPAW simulated ^{13}C spectrum for both conformations of the disordered cyclopropyl group.

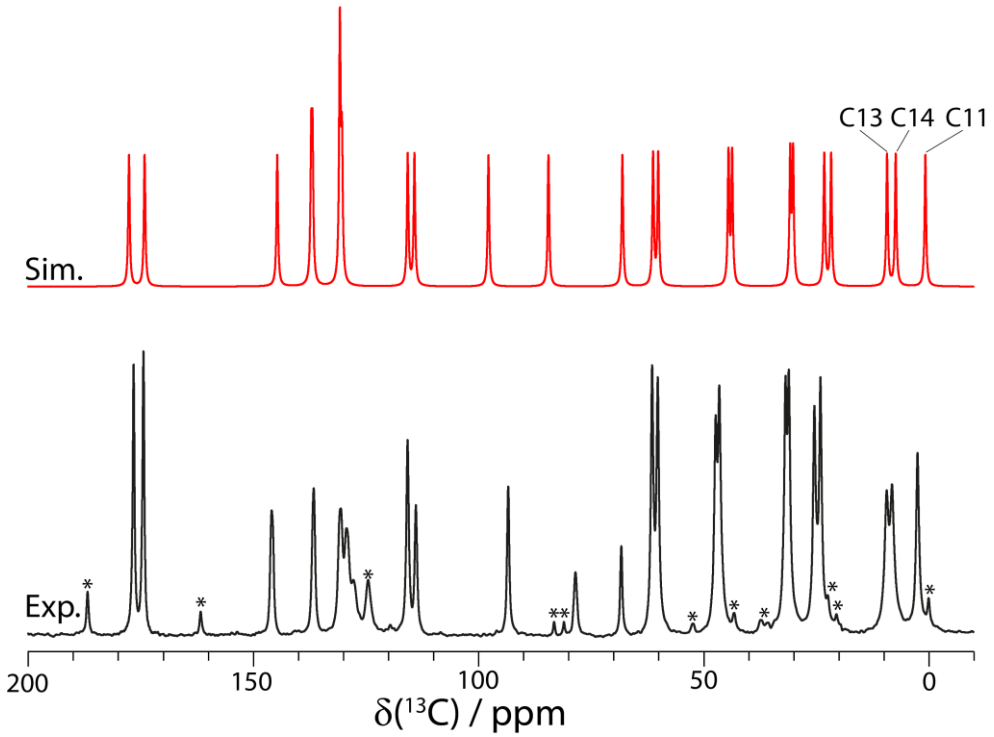

Figure S24. ^{13}C solid-state NMR spectra of **1e** and the GIPAW simulated ^{13}C spectrum for both conformations of the disordered cyclopropyl group.

^{19}F GIPAW Simulations.

In **1**, two ^{19}F signals have been observed with an intensity ratio of 1:2, with the higher intensity being assigned by GIPAW calculation to two overlapping signals (see Figure S25). In the case of **1a**, the two ^{19}F peaks observed experimentally are in excellent agreement with the GIPAW calculation (see Figure S26). While there are two molecules in the structure of **1b**, **1c**, and **1d**, only a single peak has been observed in the experimental ^{19}F spectrum, with the GIPAW calculations suggesting only small differences in the chemical shifts between the two unique molecules (see Figure S27 to Figure S29). In **1e**, a single ^{19}F peak is observed in the spectrum, supporting a *Z*' of 1 and the X-ray crystal structure (see Figure S30).

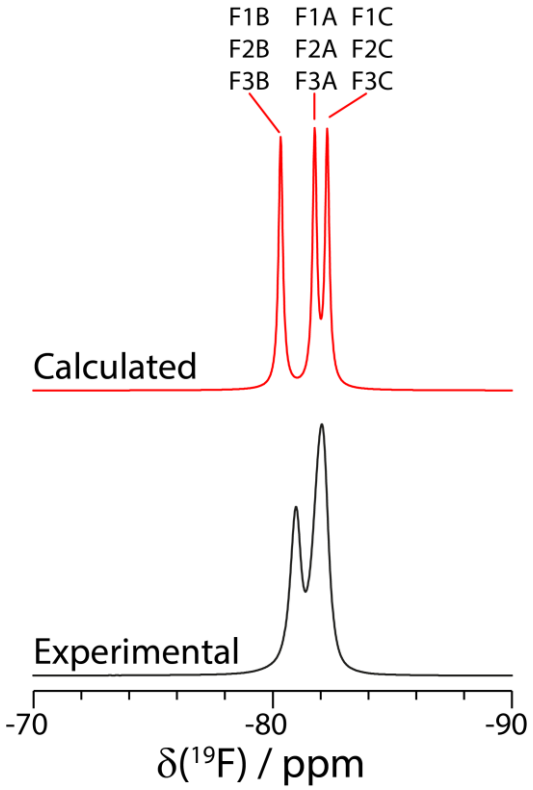

Figure S25. Experimental (black) and DFT-calculated (red) ^{19}F solid-state NMR spectrum of **1**. The experimental spectrum was acquired at 24ºC. The chemical shifts were averaged between the three fluorine atoms on the same CF_3 group, and a σ_{ref} of 145.6 ppm was used to reference the calculated chemical shifts. The labels above the calculated spectrum denote the crystallographic labels assigned to the resonance.

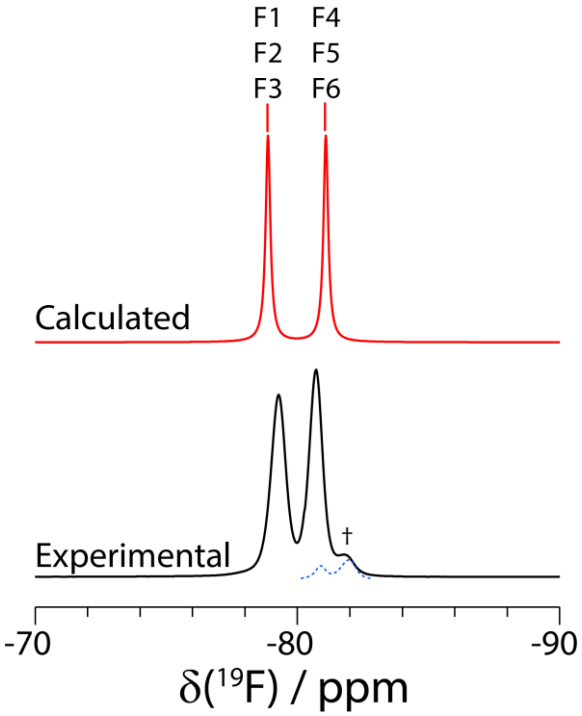

Figure S26. Experimental (black) and DFT-calculated (red) ^{19}F solid-state NMR spectrum of **1a**. The experimental spectrum was acquired at 24ºC. The dagger and the dashed blue line denotes a trace amount of starting material (**1**). The chemical shifts were averaged between the three fluorine atoms on the same CF_3 group, and a σ_{ref} of 146.9 ppm was used to reference the calculated chemical shifts. The labels above the calculated spectrum denote the assigned crystallographic sites.

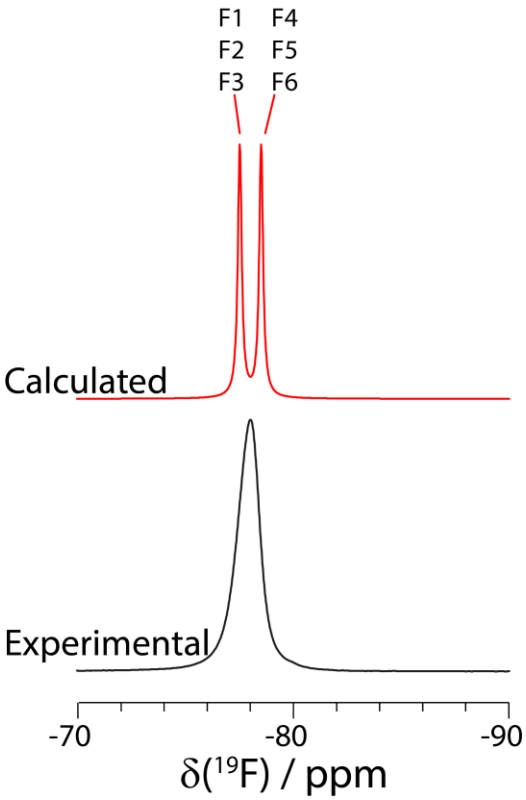

Figure S27. Experimental (black) and DFT-calculated (red) ^{19}F solid-state NMR spectrum of **1b**. The experimental spectrum was acquired at 38ºC. The calculated chemical shifts were averaged between the three fluorine atoms on the same CF_3 group, and a σ_{ref} of 146.5 ppm was used to reference the calculated chemical shifts. The labels above the calculated spectrum denote the crystallographic labels assigned to the resonance.

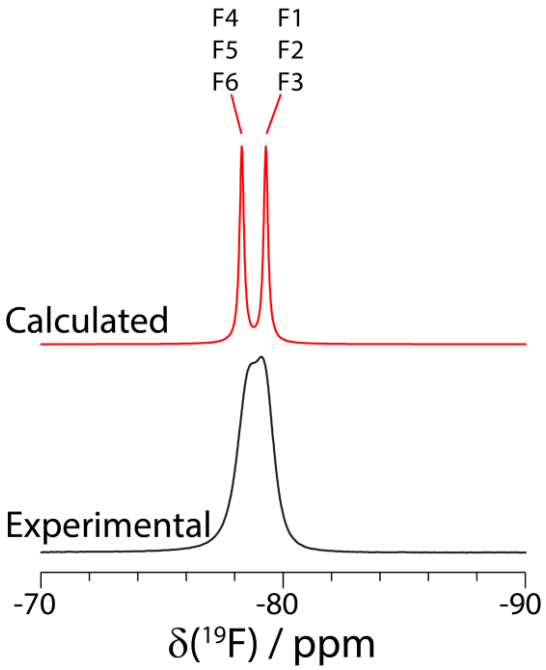

Figure S28. Experimental (black) and DFT-calculated (red) ^{19}F solid-state NMR spectrum of **1c**. The experimental spectrum was acquired at 24ºC. The calculated chemical shifts were averaged between the three fluorine atoms on the same CF_3 group, and a σ_{ref} of 145.5 ppm was used to reference the calculated chemical shifts. The labels above the calculated spectrum denote the crystallographic labels assigned to the resonance.

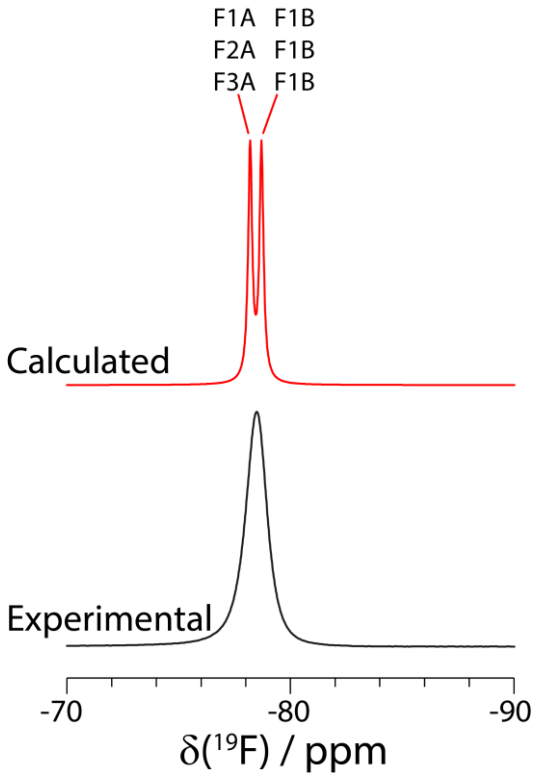

Figure S29. Experimental (black) and DFT-calculated (red) ^{19}F solid-state NMR spectrum of **1d**. The experimental spectrum was acquired at 24ºC. The calculated chemical shifts were averaged between the three fluorine atoms on the same CF_3 group, and a σ_{ref} of 144.2 ppm was used to reference the calculated chemical shifts. The labels above the calculated spectrum denote the crystallographic labels assigned to the resonance.

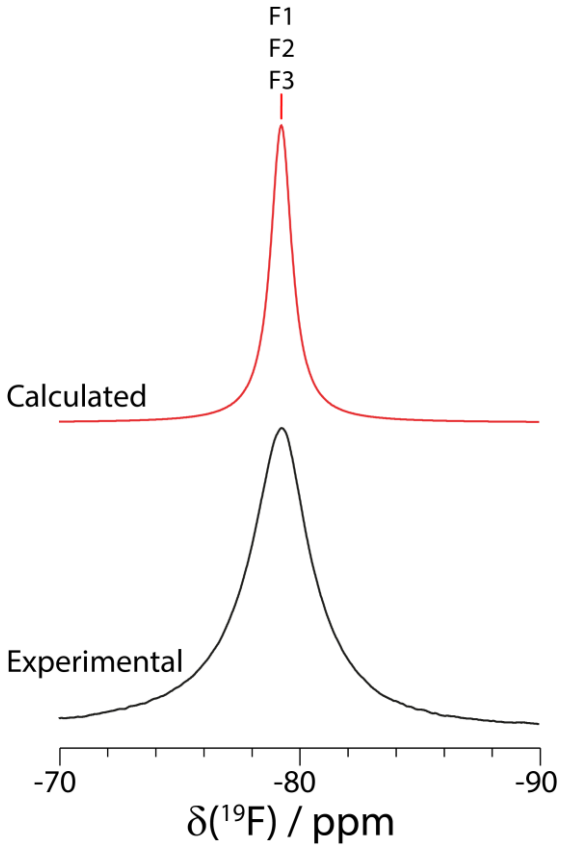

Figure S30. Experimental (black) and DFT-calculated (red) ^{19}F solid-state NMR spectrum of **1e**. The experimental spectrum was acquired at 27ºC. The chemical shifts were averaged between the three fluorine atoms on the same CF_3 group, and a σ_{ref} of 145.0 ppm was used to reference the calculated chemical shifts. The labels above the calculated spectrum denote the crystallographic labels assigned to the resonance.

T_1 relaxation times.

Table S2. $T_1(^{13}C)$ relaxation times of select resonances in compound **1**. Errors are estimated to be ±10%.

	$T_1(^{13}C)$ / s					
temperature	8.8 ppm (CH_2)	8.0 ppm (CH_2)	7.4 ppm (CH_2)	-1.0 ppm (CH)	-1.9 ppm (CH)	122.8 ppm[a] (CF_3)
3	0.2	1.2	1.3	1.8	1.7	n/a
10	0.3	1.4	1.5	1.9	1.8	2.5
17	0.5	1.5	1.6	1.9	2.0	2.3
24	0.5	1.5	1.7	1.9	2.0	2.0
31	0.7	1.7	1.8	1.9	2.1	1.9
38	0.8	1.8	1.9	1.9	2.2	1.4
45	0.9	1.8	2.0	2.0	2.3	1.5

[a] Obtained using ^{19}F-^{13}C cross-polarization.

Table S3. $T_1(^{19}F)$ relaxation times of select resonances in compound **1**. Errors are estimated to be ±10%.

	$T_1(^{19}F)$ / s	
temperature	-80.6 ppm	-81.7 ppm
3	0.60	0.60
10	0.57	0.57
17	0.53	0.53
24	0.49	0.49
31	0.45	0.44
38	0.42	0.41
45	0.38	0.37

Table S4. $T_1(^{13}C)$ and $T_1(^{19}F)$ relaxation times of select resonances in compound **1a**. Errors are estimated to be ±10%.

	$T_1(^{13}C)$ / s		$T_1(^{19}F)$ / s	
temperature	9.6 ppm	-0.35 ppm	-77.8 ppm	-79.7 ppm
3	7.9	16.5	1.04	1.04
10	10.3	22.0	1.13	1.12
17	10.4	24.4	1.22	1.20
24	10.3	24.4	1.33	1.29
31	11.2	25.6	1.45	1.38
38	12.4	25.4	1.58	1.50
45	12.7	25.4	1.71	1.58

Table S5. $T_1(^{13}C)$ and $T_1(^{19}F)$ relaxation times of select resonances in compound **1b**. Errors are estimated to be ±10%.

	$T_1(^{13}C)$ / s		$T_1(^{19}F)$ / s
temperature	8.7 ppm	-0.1 ppm	-78.0 ppm
3	53	93	13.5
10	52	103	9.9
17	60	104	7.2
24	53	106	5.8
31	56	121	4.8
38	55	101	4.0
45	50	108	3.2

Table S6. $T_1(^{13}C)$ and $T_1(^{19}F)$ relaxation times of select resonances in compound **1c**. Errors are estimated to be ±10%.

	$T_1(^{13}C)$ / s		$T_1(^{19}F)$ / s
temperature	8.5 ppm	0.1 ppm	-78.8 ppm
3	26	55	8.5
10	27	63	6.8
17	28	80	5.3
24	34	80	4.1
31	34	91	3.0
38	37	95	2.5
45	32	75	2.2

Table S7. $T_1(^{13}C)$ and $T_1(^{19}F)$ relaxation times of select resonances in compound **1d**. Errors are estimated to be ±15%.

	$T_1(^{13}C)$ / s		$T_1(^{19}F)$ / s
temperature	8.6 ppm	-0.1 ppm	-78.4 ppm
3	41	77	12.8
10	41	68	9.1
17	47	88	7.4
24	49	91	5.9
31	48	104	4.8
38	47	107	3.9
45	46	103	3.2

Table S8. $T_1(^{13}C)$ and $T_1(^{19}F)$ relaxation times of select resonances in compound **1e**. Errors are estimated to be ±10%.

	$T_1(^{13}C)$ / s			$T_1(^{19}F)$ / s
temperature	9.4 ppm	8.2 ppm	2.5 ppm	-79.1 ppm
4.7	314	299	372	44.1
12.0	320	356	414	40.7
15.3	311	292	394	37.0
18.0	n/a	n/a	n/a	41.0
21.2	282	295	398	37.0
30.9	296	290	382	30.0
37.9	285	311	393	26.3

***T_1* fitting parameters.**

Table S9. Detailed $T_1(^{13}C)$ fitting parameters of the CH_2 carbon atoms of the cyclopropyl group.

compound	peak	site[a]	E_a kJ mol^{-1}	τ_0 (s)	S^2
1	8.8 ppm	C17A C18A C17B C18B[b]	12 ± 2	(2.4 ± 0.8) x10^{-13}	0.60
	8.0 ppm	C13A C14A	10 ± 2	(2.3 ± 0.8) x10^{-13}	0.60
	7.4 ppm	C13B C14B	11 ± 2	(1.3 ± 0.5) x10^{-13}	0.60
1a	9.8 ppm	C13 C14 C27 C28	8 ± 2	(1.1 ± 0.3) x10^{-13}	0.20[c]
1b	8.7 ppm	C21 C22 C31 C32 C51 C52 C61 C62[b]	2 ± 1	(2.5 ± 0.5) x10^{-13}	0.25
1c	8.6 ppm	C13A C14A C13B C13D C14B C14D[b]	4 ± 2	(2.0 ± 0.7) x10^{-13}	0.28
1d	8.5 ppm	C13B C14B	3 ± 1	(1.9 ± 0.3) x10^{-13}	0.20[c]
1e	8.2 ppm	C13 C14	1 ± 1	(7 ± 1) x10^{-14}	0.20[c]

[a] Crystallographic site assigned using GIPAW calculations.

[b] Disordered over two positions.

[c] S^2 fixed to 0.2.

Characterization of the rocking motion in 1.

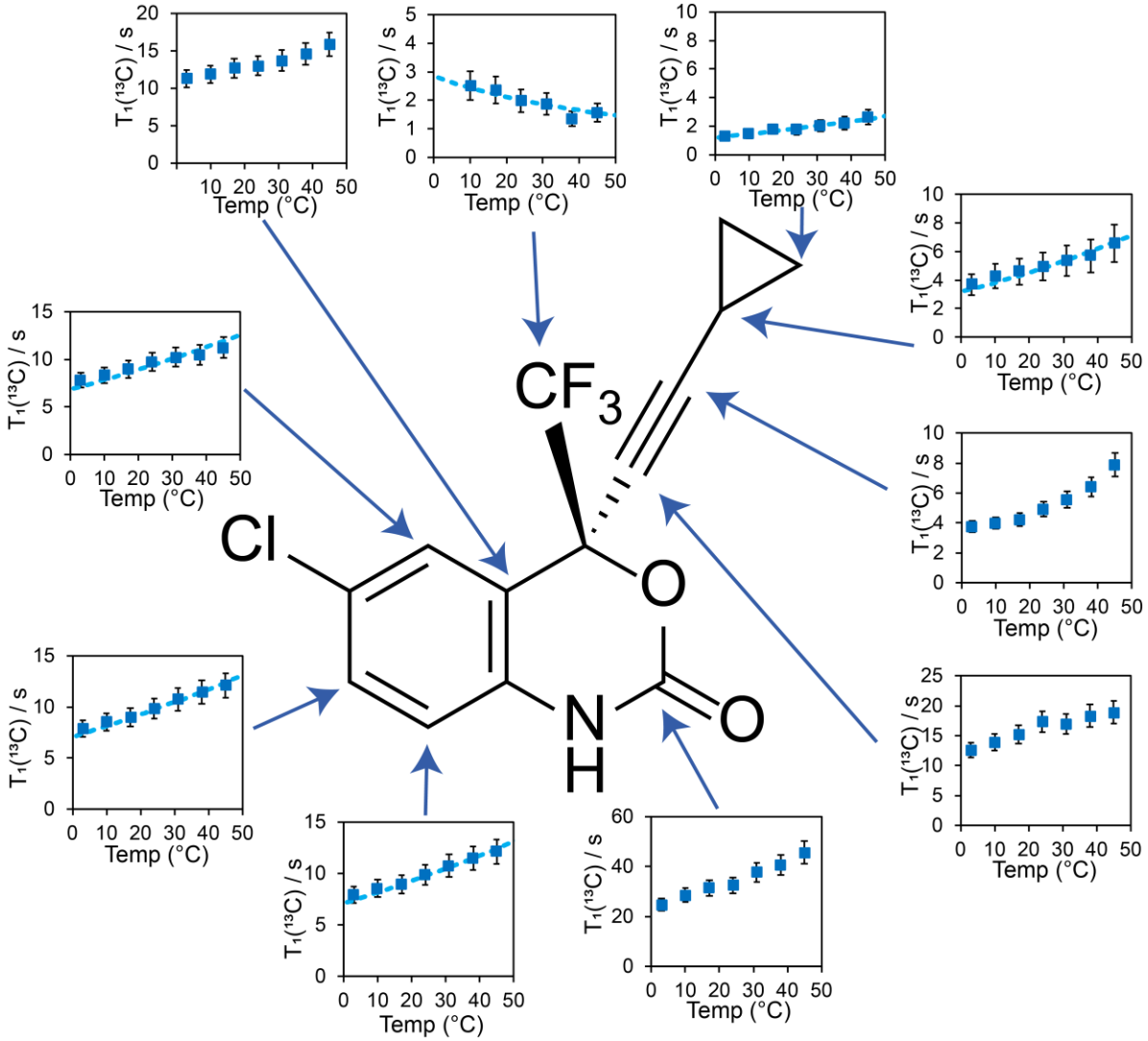

Figure S31. $T_1(^{13}C)$ relaxation times of selected carbon atoms in **1**. The $T_1(^{13}C)$ of the cyclopropyl group have been assigned to disordered group in the structure (atoms C16A C17A C18A / C16B C17B C18A). Lines of best fit using Eq S7 are shown for the CH, CH_2, and CF_3 carbons. The fitting parameters can be found in Table S11.

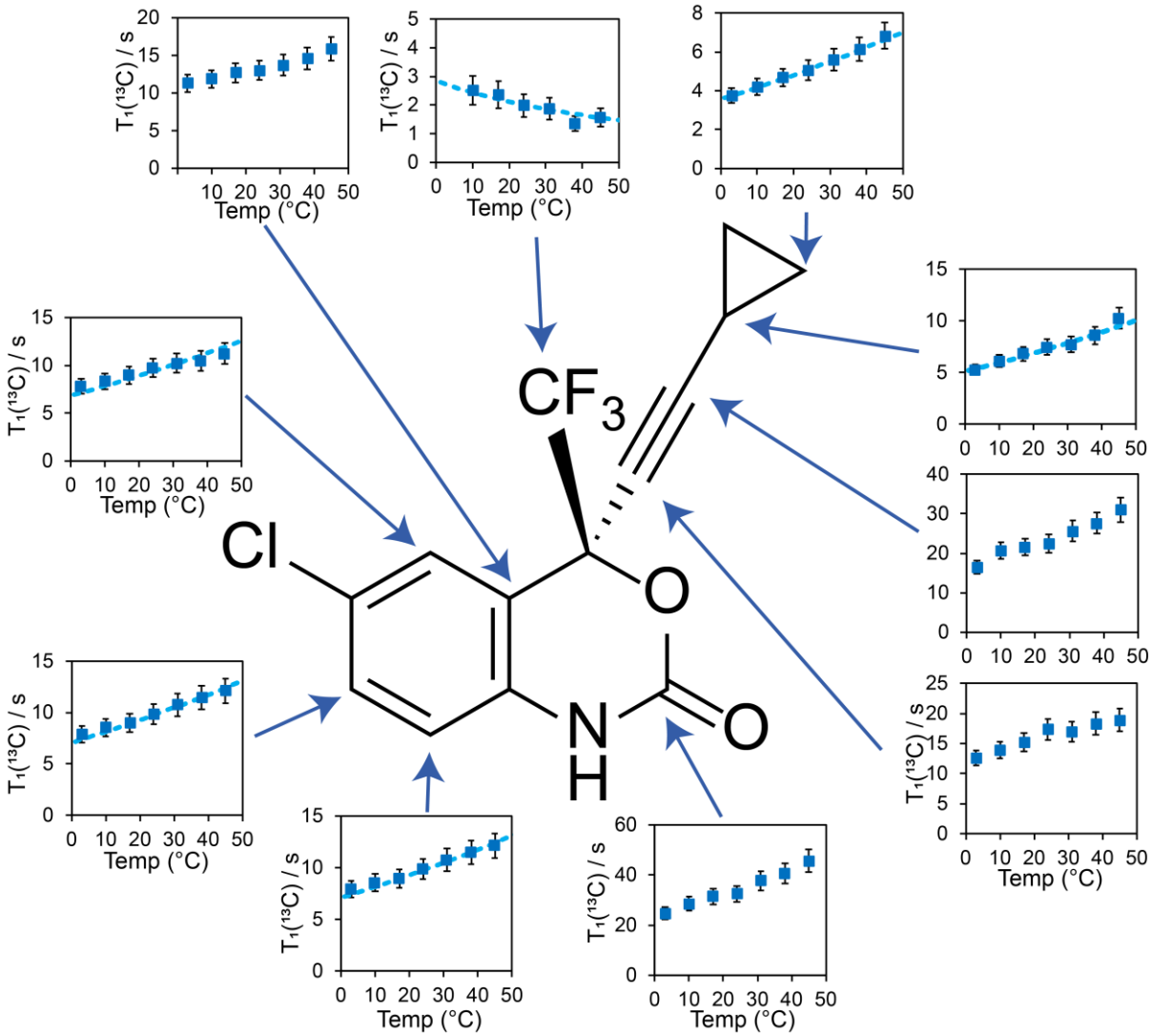

Figure S32. $T_1(^{13}C)$ relaxation times of selected carbon atoms in **1**. The $T_1(^{13}C)$ of the cyclopropyl group have been assigned to ordered group in the structure (atoms C12A C13A C14A). Lines of best fit using Eq S7 are shown for the CH, CH_2, and CF_3 carbons. The fitting parameters can be found in Table S11.

Table S10. Detailed $T_1(^{13}C)$ fitting parameters of selected protonated carbon atoms in **1**, as shown in Figures S31 and S32.

chemical shift	crystallographic assignment	Ea kJ mol^{-1}	τ_0 (s)	S^2
-1.9 ppm	C12A & C12B[a]	10 ± 2	(2.7 ± 1.0) x10^{-13}	0.6
-1.0 ppm	C16A / C16B[b]	12 ± 2	(2.0 ± 0.5) x10^{-13}	0.6
7.4 ppm	C13B C14B	11 ± 2	(1.3 ± 0.5) x10^{-13}	0.6
8.0 ppm	C13A C14A	10 ± 2	(2.3 ± 0.8) x10^{-13}	0.6
8.8 ppm	C17A C18A / C17B C18B[b]	12 ± 2	(2.4 ± 0.8) x10^{-13}	0.6
119 ppm	C6A & C6B & C6C[a]	9 ± 1	(1.1 ± 0.3) x10^{-13}	0.1[c]
127 ppm	C3A & C3B & C3C[a]	9 ± 1	(1.5 ± 0.3) x10^{-13}	0.1[c]
133 ppm	C5A & C5B & C5C[a]	9 ± 1	(1.4 ± 0.3) x10^{-13}	0.1[c]

[a] Overlap of multiple crystallographic sites in the NMR spectrum. [b] Disordered position.
[c] S^2 assumed to be 0.1.

Table S11. $T_1(^{13}C)$ of selected aromatic C-H carbons of Efavirenz in **1** and cocrystals **1a** – **1e**.

	1a (131 ppm) / s	**1b**[a] / s	**1c**[a] / s	**1d**[a] / s
276.0	57	>200	>200	>200
283.0	123	>200	>200	>200
290.0	109	>200	>200	>200
297.0	131	>200	>200	>200
304.0	101	>200	>200	>200
311.0	104	>200	>200	>200
318.0	92	>200	>200	>200
	1e (115 ppm) / s			
277.9	253			
285.1	248			
288.3	260			
291.2	249			
294.9	249			
304.0	262			
311.0	260			

[a] Precise values could not be obtained due to the long $T_1(^{13}C)$.

Thermogravimetric analysis.

Table S12. Thermogravimetric analysis of **1** and cocrystals **1a** – **1e** after 12 months of storage at room temperature, reporting the onset and peak melting temperatures. Two trials were performed for each sample.

	replicate 1				replicate 2			
	melt 1		melt 2		melt 1		melt 2	
sample	onset / °C	peak / °C	onset / °C	peak / °C	onset / °C	peak / °C	onset / °C	peak / °C
1	137.2	138.9			137.1	138.8		
1a	73.1	74.9			73.1	74.8		
1b	115.9	117.3			115.9	117.3		
1c[a]	87.8	89.4	119.1	120.6	87.7	89.4	118.9	120.8
1d[a]	110.5	112.4	123.8	126.2	110.6	112.5	124.0	126.5
1e	160.1	164.1			160.1	164.0		

[a] Two melts have been measured likely due to sample decomposition over the storage time.

Section III – Computational Results.

A) Interactions energies involving the cyclopropyl group

Table S13. Crystal Interactions analysis of **1** for crystallographic site 1 (C16A / C16B, C17A / C17B, C18A / C18B).

#	Description	Energy in the relaxed state (kJ mol^{-1})	Symmetry operation
1	Ef1···Ef1	-42.5	1-x, -y, 1+z
2	Ef1···Ef1	-5.5	1-x, -y, 1+z
3	Ef1···Ef3	-43.0	½-x, ½+y, 2-z
4	Ef1···Ef3	-0.3	1-x, -y, z
5	Ef1···Ef2	-4.0	1-x, -y, z
	Total	-95.3	

[a] Ef1 corresponds to the molecule with atoms C16A/C16B, C17A/C17B, C18A/C18B, Ef2 corresponds to the molecule with atoms C12A, C13A, C14A, and Ef2 corresponds to the molecule with atoms C12A, C13A, C14A.

Table S14. Crystal Interactions analysis of **1** for crystallographic site 2 (C12A, C13A, C14A).

#	Description[a]	Energy in the relaxed state (kJ mol^{-1})	Symmetry operation
1	Ef2···Ef1	-41.0	x, y, 1+z
2	Ef2···Ef1	-4.0	1-x, -y, z
3	Ef2···Ef2	-24.0	½+x, ½-y, 2-z
4	Ef2···Ef3	-49.7	x, y, z
5	Ef2···Ef3	-23.6	x, y, -1+z
	Total	-142.3	

[a] Ef1 corresponds to the molecule with atoms C16A/C16B, C17A/C17B, C18A/C18B, Ef2 corresponds to the molecule with atoms C12A, C13A, C14A, and Ef2 corresponds to the molecule with atoms C12A, C13A, C14A.

Table S15. Crystal Interactions analysis of **1** for crystallographic site 3 (C12B, C13B, C14B).

#	Description[a]	Energy in the relaxed state (kJ mol^{-1})	Symmetry operation
1	Ef3···Ef1	-25.8	x, y, z
2	Ef3···Ef1	-0.3	1-x, -y, z
3	Ef3···Ef2	-49.7	x, y, z
4	Ef3···Ef2	-23.6	x, y, 1+z
	Total	-99.4	

[a] Ef1 corresponds to the molecule with atoms C16A/C16B, C17A/C17B, C18A/C18B, Ef2 corresponds to the molecule with atoms C12A, C13A, C14A, and Ef2 corresponds to the molecule with atoms C12A, C13A, C14A.

Table S16. Crystal Interactions analysis of **1a** for crystallographic site 1 (C22, C23, C24).

#	Description[a]	Energy in the relaxed state (kJ mol^{-1})	Symmetry operation
1	Ef1···Ef2	-84.0	x, 1+y, z
2	Ef1···Ef2	-16.0	1-x, 1+y, 1-z
3	Ef1···Ef2	-2.7	1-x, 2+y, 1-z
4	Ef1···Ef2	-14.8	-1/2+x, ½+y, z
5	Ef1···Ef2	-33.5	-1/2+x, 3/2+y, z
6	Ef1···Ef1	-11.8	x, 1+y, z
7	Ef1···Ef1	-1.1	-1/2+x, ½+y, z
	Total	-163.9	

[a] Ef1 corresponds to the molecule with atoms C22, C23, C24, whereas Ef2 corresponds to the molecule with atoms C26, C27, C28.

Table S17. Crystal Interactions analysis of **1a** for crystallographic site 2 (C26, C27, C28).

#	Description[a]	Energy in the relaxed state (kJ mol^{-1})	Symmetry operation
1	Ef2···Ef2	-7.9	x, 1+y, z
2	Ef2···Ef2	-22.5	1-x, y, 1-z
3	Ef2···Ef2	-5.6	1-x, 1+y, 1-z
4	Ef2···Ef2	-3.0	½+x,
5	Ef2···Ef2	-14.6	3/2-x, ½+y, 1-z
6	Ef2···Ef2	-14.6	3/2-x, -1/2+y, 1-z
7	Ef2···Ef1	-16.0	1-x, 1+y, 1-z
8	Ef2···Ef1	-2.7	1-x, 2+y, 1-z
9	Ef2···Ef1	-33.5	-1/2+x, 3/2+y, z
	Total	-120.4	

[a] Ef1 corresponds to the molecule with atoms C22, C23, C24, whereas Ef2 corresponds to the molecule with atoms C26, C27, C28.

Table S18. Crystal Interactions analysis of **1b** for crystallographic site 1 (C41, C51, C61).

#	Description[a]	Energy in the relaxed state (kJ mol^{-1})	Symmetry operation
1	Ef1···Ef1	-31.3	x, 1+y, z
2	Ef1···Ef1	-64.6	1+x, y, z
3	Ef1···Ef1	-8.3	1+x, -1+y, z
4	Ef1···Ef2	-17.9	x, y, z
5	Ef1···Ef2	-6.9	1+x, y, z
6	Ef1···Ef2	-18.7	-1+x, y, z
7	Ef1···Ef2	-1.5	-1+x. -1+y, z
	Total	-149.2	

[a] Ef1 corresponds to the molecule with atoms C41, C51, C61, whereas Ef2 corresponds to the molecule with atoms C11, C21, C31

Table S19. Crystal Interactions analysis of **1b** for crystallographic site 2 (C11, C21, C31).

#	Description[a]	Energy in the relaxed state (kJ mol^{-1})	Symmetry operation
1	Ef2···Ef1	-17.9	x, y, z
2	Ef2···Ef1	-18.7	-1+x, y, z
3	Ef2···Ef1	-1.5	-1+x, -1+y, z
4	Ef2···Ef1	-6.6	-2+x, y, z
5	Ef2···Ef2	-57.1	1+x, y, z
6	Ef2···Ef2	-33.2	1+x, 1+y, z
7	Ef2···Ef2	-7.5	2+x, 1+y, z
	Total	-142.5	

[a] Ef1 corresponds to the molecule with atoms C41, C51, C61, whereas Ef2 corresponds to the molecule with atoms C11, C21, C31

Table S20. Crystal Interactions analysis of **1c** for crystallographic site 1 (C12A, C13A, C14A).

#	Description[a]	Energy in the relaxed state (kJ mol^{-1})	Symmetry operation
1	Ef1···Ef2	-14.6	x, y, z
2	Ef1···Ef2	-14.5	1+x, y, z
3	Ef1···Ef2	-2.6	-1+x, 1+y, z
4	Ef1···Ef2	-7.6	-2+x, y, z
5	Ef1···Ef1	-30.0	x, 1+y, z
6	Ef1···Ef1	-67.6	1+x, y, z
7	Ef1···Ef1	-8.9	1+x, 1+y, z
	Total	-145.8	

[a] Ef1 corresponds to the molecule with atoms C12A, C13A, C14A, whereas Ef2 corresponds to the molecule with atoms C12B, C13B, C14B

Table S21. Crystal Interactions analysis of **1c** for crystallographic site 2 (C12B, C13B, C14B).

#	Description[a]	Energy in the relaxed state (kJ mol^{-1})	Symmetry operation
1	Ef2···Ef2	-66.6	1+x, y, z
2	Ef2···Ef2	-29.7	1+x, -1+y, z
3	Ef2···Ef2	-6.9	2+x, -1+y, z
4	Ef2···Ef1	-14.6	x, y, z
5	Ef2···Ef1	-14.5	1+x, y, z
6	Ef2···Ef1	-2.6	1+x, -1+y, z
7	Ef2···Ef1	-7.6	-1+x, y, z
	Total	-142.5	

[a] Ef1 corresponds to the molecule with atoms C12A, C13A, C14A, whereas Ef2 corresponds to the molecule with atoms C12B, C13B, C14B

Table S22. Crystal Interactions analysis of **1d** for crystallographic site 1 (C12A, C13A, C14A).

#	Description[a]	Energy in the relaxed state (kJ mol^{-1})	Symmetry operation
1	Ef1···Ef1	-69.7	1+x, y, z
2	Ef1···Ef1	-28.9	1+x, -1+y, z
3	Ef1···Ef1	-8.8	2+x, -1+y, z
4	Ef1···Ef2	-15.9	1+x, y, z
5	Ef1···Ef2	-15.9	2+x, y, z
6	Ef1···Ef1	-2.3	2+x, -1+y, z
7	Ef1···Ef1	-7.7	3+x, y, z
	Total	-149.2	

[a] Ef1 corresponds to the molecule with atoms C12A, C13A, C14A, whereas Ef2 corresponds to the molecule with atoms C12B, C13B, C14B

Table S23. Crystal Interactions analysis of **1d** for crystallographic site 2 (C12B, C13B, C14B).

#	Description[a]	Energy in the relaxed state (kJ mol^{-1})	Symmetry operation
1	Ef2···Ef1	-7.8	x, y, z
2	Ef2···Ef1	-15.9	1+x, y, z
3	Ef2···Ef1	-15.9	2+x, y, z
4	Ef2···Ef1	-2.3	2+x, -1+y, z
5	Ef2···Ef2	-28.4	x, 1+y, z
6	Ef2···Ef2	-71.5	1+x, y, z
7	Ef2···Ef2	-8.8	1+x, 1+y, z
	Total	-150.6	

[a] Ef1 corresponds to the molecule with atoms C12A, C13A, C14A, whereas Ef2 corresponds to the molecule with atoms C12B, C13B, C14B

Table S24. Crystal Interactions analysis of **1e**.

#	Description[a]	Energy in the relaxed state (kJ mol^{-1})	Symmetry operation
1	Ef···Ef	-55.8	x, y, 1+z
2	Ef···Ef	-55.8	x, y, -1+z
3	Ef···Ef	-40.7	3/2-x, 1-y, ½+z
4	Ef···Ef	-40.7	3/2-x, 1-y, -½+z
5	Ef···Ef	-21.0	½-x, 1-y,
6	Ef···Ef	-4.3	½-x, 1-y, 3/2+z
	Total	218.3	

B) Interactions energies involving the CF_3 group

Table S25. Crystal Interactions analysis of **1** for crystallographic site 1 (F1A F2A F3A).

#	Description[a]	Energy in the relaxed state (kJ mol^{-1})	Symmetry operation
1	Ef1···Ef1	-8.6	x, y, 1+z
2	Ef1···Ef1	-24.0	½ + x, ½ - y, 2-z
3	Ef1···Ef2	-49.7	x, y, z
4	Ef1···Ef2	-23.6	x, y, -1+z
5	Ef1···Ef2	-38.2	½+x, ½-y, 2-z
	Total	-144.1	

[a] Ef1 corresponds to the molecule with atoms F1A, F2A, F3A. Ef2 corresponds to the molecule with atoms F1B, F2B, F3B. Ef3 corresponds to the molecule with atoms F1C, F2C, F3C.

Table S26. Crystal Interactions analysis of **1** for crystallographic site 2 (F1C F2C F3C).

#	Description[a]	Energy in the relaxed state (kJ mol^{-1})	Symmetry operation
1	Ef3···Ef3	-11.4	x, y, 1+z
2	Ef3···Ef3	-42.5	1-x, -y, z
3	Ef3···Ef2	-25.8	x, y, z
4	Ef3···Ef1	-39.0	x, y, z
5			
	Total	-118.7	

[a] Ef1 corresponds to the molecule with atoms F1A, F2A, F3A. Ef2 corresponds to the molecule with atoms F1B, F2B, F3B. Ef3 corresponds to the molecule with atoms F1C, F2C, F3C.

Table S27. Crystal Interactions analysis of **1** for crystallographic site 3 (F1B F2B F3B).

#	Description[a]	Energy in the relaxed state (kJ mol^{-1})	Symmetry operation
1	Ef2···Ef3	-29.6	½-x, ½+y, 1-z
2	Ef2···Ef2	-13.2	x, y, 1+z
3	Ef2···Ef2	-49.7	x, y, z
4	Ef2···Ef1	-38.1	-1/2+x, ½-y, 1-z
5			
	Total	-130.6	

[a] Ef1 corresponds to the molecule with atoms F1A, F2A, F3A. Ef2 corresponds to the molecule with atoms F1B, F2B, F3B. Ef3 corresponds to the molecule with atoms F1C, F2C, F3C.

Table S28. Crystal Interactions analysis of **1b** for crystallographic site 1 (F1AA F2AA F4A).

#	Description[a]	Energy in the relaxed state (kJ mol^{-1})	Symmetry operation
1	Ef1···Ef1	-31.3	x, 1+y, z
2	Ef1···Ef1	-64.6	1+x, y, z
3	Ef1···Ef1	-3.2	1+x, 1+y, z
4	Ef1···Bipy	-38.5	x, y, 1+z
5	Ef1···Bipy	-14.6	-1+x, y, 1+z
	Total	-152.2	

[a] Ef1 corresponds to the molecule with atoms F1 F2 F3.

Table S29. Crystal Interactions analysis of **1b** for crystallographic site 2 (F3AA F0AA F).

#	Description[a]	Energy in the relaxed state (kJ mol^{-1})	Symmetry operation
1	Ef2···Ef2	-3.7	x, 1+y, z
2	Ef2···Ef2	-57.1	1+x, y, z
3	Ef2···Ef2	-33.2	1+x, 1+y, z
4	Ef2···Bipy	-18.4	x, y, z
5	Ef2···Bipy	-32.4	1+x, y, z
	Total	-144.8	

[a] Ef2 corresponds to the molecule with atoms F4 F5 F6.

Table S30. Crystal Interactions analysis of **1c** for crystallographic site 1 (F1A F2A F3A).

#	Description[a]	Energy in the relaxed state (kJ mol^{-1})	Symmetry operation
1	Ef1···Ef1	-4.7	x, 1+y, z
2	Ef1···Ef1	-66.6	1+x, y, z
3	Ef1···Ef1	-29.7	1+x, -1+y, z
4	Ef1···Bipy	-28.2	x, y, 1+z
5	Ef1···Bipy	-28.0	1+x, y, 1+z
	Total	-157.2	

[a] Ef1 corresponds to the molecule with atoms F1 F2 F3.

Table S31. Crystal Interactions analysis of **1c** for crystallographic site 1 (F1B F2B F3B).

#	Description[a]	Energy in the relaxed state (kJ mol^{-1})	Symmetry operation
1	Ef2···Ef2	-30.0	x, 1+y, z
2	Ef2···Ef2	-67.6	1+x, y, z
3	Ef2···Ef2	-2.3	1+x, -1+y, z
4	Ef2···Bipy	-41.1	x, y, z
5	Ef2···Bipy	-12.5	-1+x, y, z
	total	-153.5	

[a] Ef2 corresponds to the molecule with atoms F4 F5 F6.

Table S32. Crystal Interactions analysis of **1d** for crystallographic site 1 (F1A F2A F3A).

#	Description[a]	Energy in the relaxed state (kJ mol^{-1})	Symmetry operation
1	Ef1···Ef1	-69.7	1+x, y, z
2	Ef1···Ef1	-28.9	1+x, -1+y, z
3	Ef1···Bipy	-31.0	x, y, z
4	Ef1···Bipy	-17.2	-1+x, y, z
	total	-146.8	

[a] Ef1 corresponds to the molecule with atoms F1 F2 F3.

Table S33. Crystal Interactions analysis of **1d** for crystallographic site 2 (F1B F2B F3B).

#	Description[a]	Energy in the relaxed state (kJ mol^{-1})	Symmetry operation
1	Ef2···Ef2	-28.4	x, 1+y, z
2	Ef2···Ef2	-71.5	1+x, y, z
3	Ef2···Bipy	-40.5	-2+x, y, -1+z
4	Ef2···Bipy	-14.2	-3+x, y, -1+z
	total	-154.6	

[a] Ef2 corresponds to the molecule with atoms F4 F5 F6.

Table S34. Crystal Interactions analysis of **1e** for crystallographic site 1 (F1 F2 F3).

#	Description	Energy in the relaxed state (kJ mol^{-1})	Symmetry operation
1	Ef···Ef	-55.8	x, y, 1+z
2	Ef···Ef	-3.0	-1+x, y, z
3	Ef···Ef	-3.6	-1+x, y, 1+z
4	Ef···Ef	-40.7	3/2-x, 1-y, 1/2+z
5	Ef···Pro	-33.7	x, y, z
6	Ef···Pro	-19.0	x, y, -1 + z
	total	-155.8	

C) Transition state energy for the cyclopropyl group rotation

Table S35. DFT-calculated transition state barrier of the cyclopropyl group in **1**, **1b**, and **1c**.

compound	site label	Transition State Energy kJ mol^{-1}
1	C16A C17A C18A / C16B C17B C18B	8.5[a]
1b	C11 C21 C31 / C12 C22 C32	2.1
1c	C12B C13B C14B / C12D C13D C14D	5.3

[a] Performed on a reduced model.

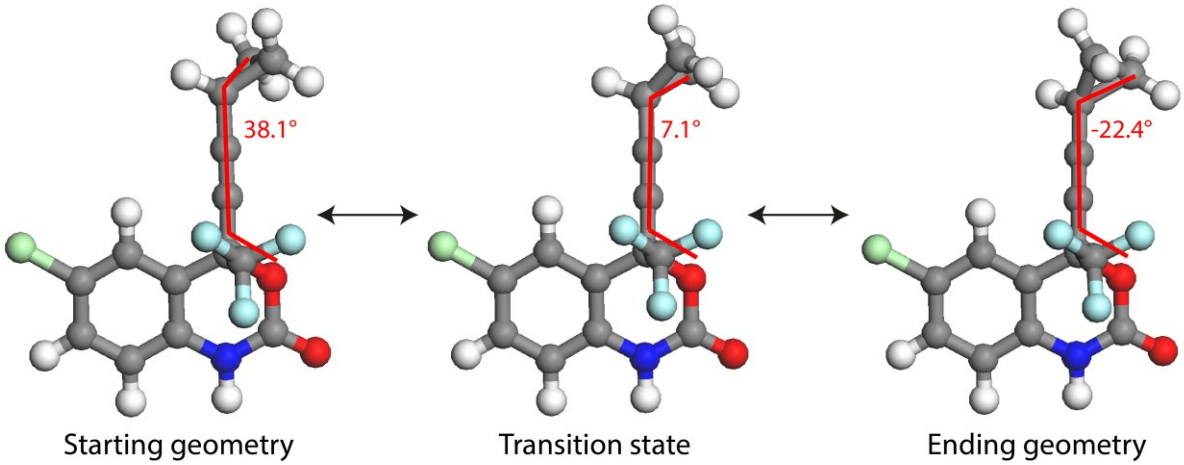

Figure S33. Starting geometry, transition state, and ending geometry of the motion of the cyclopropyl group (C11 C21 C31 / C12 C22 C32) in structure **1b**. While the structure featured periodicity, only the molecule with motion is shown here for clarity. The rotation of the cyclopropyl group is not accompanied by the bending of the ethynyl group, and only minor rocking motions of the molecule is observed. The torsion angle between the ethynyl axis and the cyclopropyl group is shown in red.

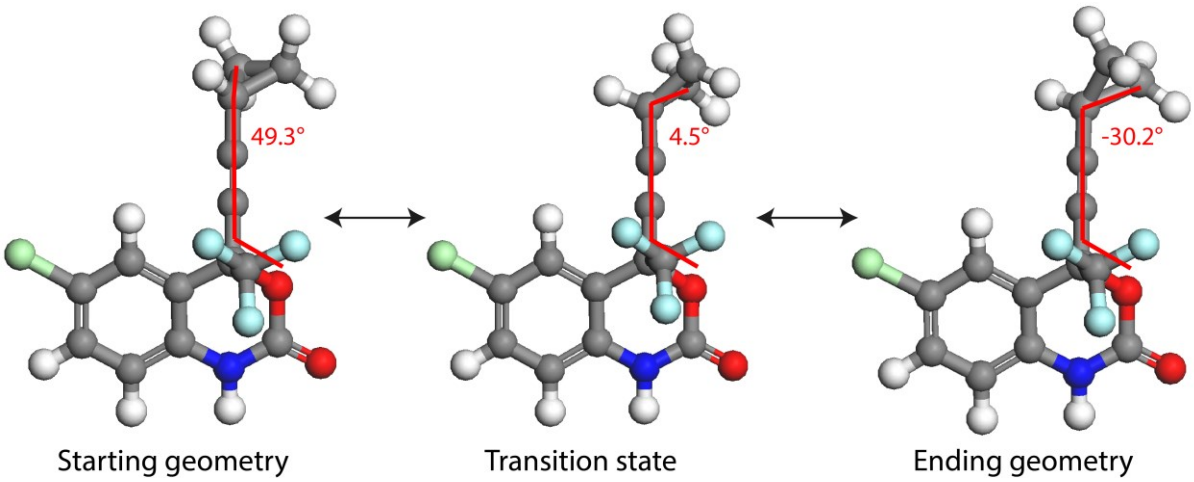

Figure S34. Starting geometry, transition state, and ending geometry of the motion of the cyclopropyl group (C12B C13B C14B / C12D C13D C14D) in structure **1c**. While the structure featured periodicity, only the molecule with motion is shown here for clarity. he rotation of the cyclopropyl group is not accompanied by the bending of the ethynyl group, and only minor rocking motions of the molecule is observed. The torsion angle between the ethynyl axis and the cyclopropyl group is shown in red.

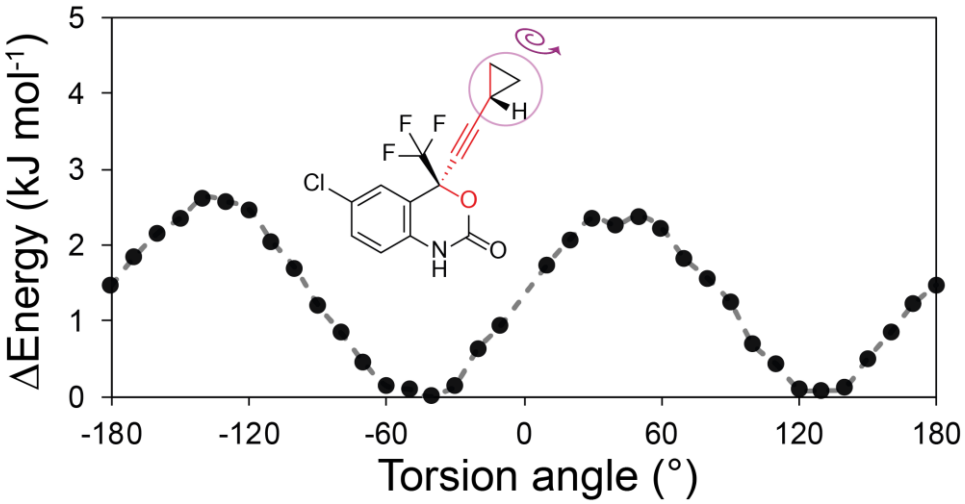

Figure S35. DFT-calculated potential energy surface of an isolated molecule of Efavirenz. The torsion angle of interest has been highlighted in red on the molecular structure.

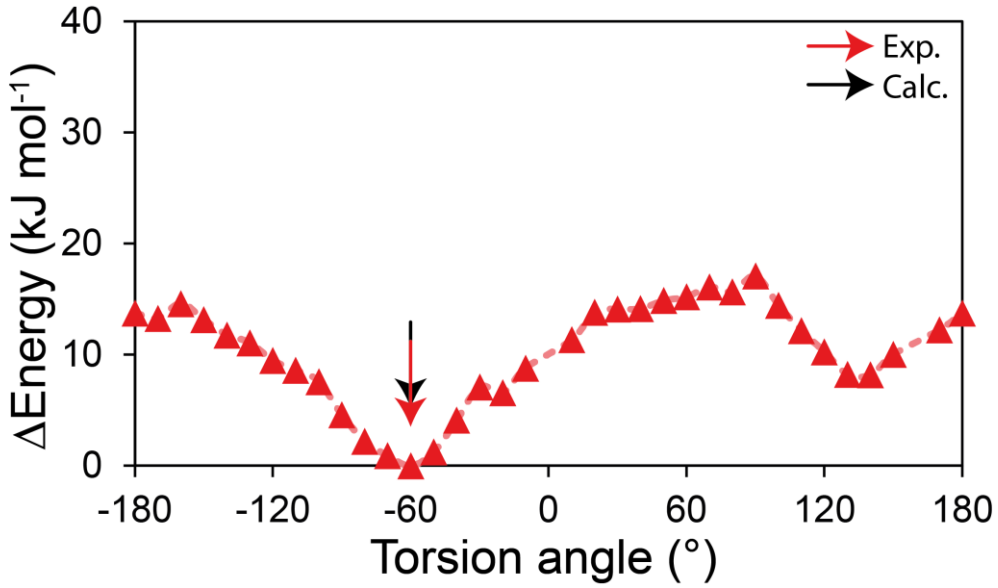

Figure S36. DFT-calculated potential energy surface for the rotation of a cyclopropyl group in **1a** (site 2), performed on a periodic model. The torsion angles from the X-ray structure (exp.) and DFT-optimized structure (calc.) are indicated by the red and black arrows, respectively. The second energy minimum at 130° may be inaccessible due to the high rotational energy barrier.[9]

Section IV – X-ray Parameters, Crystallographic Sites, and Thermal Ellipsoid Plots.

Table S36. Crystallographic assignments corresponding to the labels from Table 1 (cyclopropyl group) of the main text.

	cyclopropyl group		CF_3 group	
sample	table 1 label	crystallographic assignment	table 2 label	crystallographic assignment
1	CYP site 1	C16A C17A C18A & C16B C17B C18B[a]	CF_3 site 1	F1A F2A F3A
	CYP site 2	C12A C13A C14A	CF_3 site 2	F1C F2C F3C
	CYP site 3	C12B C13B C14B	CF_3 site 3	F1B F2B F3B
1a	CYP site 1	C22 C23 C24	CF_3 site 1	F1 F2 F3
	CYP site 2	C26 C27 C28	CF_3 site 2	F4 F5 F6
1b	CYP site 1	C41 C51 C61 & C42 C52 C62[a]	CF_3 site 1	F1AA F2AA F4A
	CYP site 2	C11 C21 C31 & C12 C22 C32[a]	CF_3 site 2	F3AA F0AA F
1c	CYP site 1	C12A C13A C14A	CF_3 site 1	F1A F2A F3A
	CYP site 2	C12B C13B C14B & C12D C13D C14D[a]	CF_3 site 2	F1B F2B F3B
1d	CYP site 1	C12A C13A C14A	CF_3 site 1	F1A F2A F3A
	CYP site 2	C12B C13B C14B	CF_3 site 2	F1B F2B F3B
1e	CYP site 1	C11 C13 C14	CF_3 site 1	F1 F2 F3

[a] Site is crystallographically disordered.

Table S37. Torsion angle $\theta_{O\text{-}C\text{-}C\text{-}C}$, as shown on Figure 1 of the main text, measured in the experimental crystal structure and DFT-optimized structure. The probe atoms defining the torsion angles are given. The experimental errors were estimated using the thermal ellipsoids.

sample	site	probe atoms	experimental $\theta_{O\text{-}C\text{-}C\text{-}C}$ (°)	DFT-optimized $\theta_{O\text{-}C\text{-}C\text{-}C}$ (°)	Transition state $\theta_{O\text{-}C\text{-}C\text{-}C}$ (°)
1	CYP site 1[a]	O2C-C2C-C16A-C18A[ab]	–42 ± 26	–22.2	45.9
		O2C-C2C-C16B-C17B[ab]	94 ± 24	99.0	
	CYP site 2	O2A-C2A-C12A-C14A	146 ± 25	130.4	n/a
	CYP site 3	O1B-C2B-C12B-C14B	–134 ± 23	–137.9	n/a
1a	CYP site 1	O3-C12-C22-C24	191 ± 31	192.7	n/a
	CYP site 2	O1-C8-C26-C28	–60 ± 19	–62.5	n/a
1b	CYP site 1[a]	O1B-C2B-C41-C51[a]	69 ± 77	169.5	n/a
		O1B-C2B-C42-C52[a]	–87 ± 46	n/a	n/a
	CYP site 2[a]	O1A-C2A-C11-C21[a]	–21 ± 27	–22.4	7.1
		O1A-C2A-C12-C22[a]	67 ± 12	38.1	
1c	CYP site 1	O1A-C2A-C12A-C14A	–34 ± 30	–36.1	n/a
	CYP site 2[a]	O1B-C2B-C12D-C14D[a]	–30 ± 23	–30.2	4.5
		O1B-C2B-C12B-C14B[a]	49 ± 31	49.3	
1d	CYP site 1	O1A-C2A-C12A-C14A	–31 ± 30	–30.9	n/a
	CYP site 2	O1B-C2B-C12B-C14B	–30 ± 38	–29.0	n/a
1e	CYP site 1	O1-C1-C11-C13	133 ± 12	136.8	n/a

[a] Site is crystallographically disordered. [b] Crystallographic label slightly differs between the two disordered positions.

Table S38. Swaying angle (θ_{sway}) of the cyclopropyl group, as shown on Figure 1 of the main text, measured in the experimental crystal structure and DFT-optimized structure. The probe atoms defining the swaying angles are given. The experimental errors were estimated using the thermal ellipsoids.

sample	site	probe atoms	experimental θ_{sway} (°)	DFT-optimized θ_{sway} (°)	Transition state θ_{sway} (°)
1	CYP site 1[a]	C9C-C2C-C16A[a]	99 ± 7	108.3	107.8
		C9C-C2C-C16B[a]	116 ± 13	113.1	
	CYP site 2	C9A-C2A-C12A	108 ± 17	106.5	n/a
	CYP site 3	C9B-C2B-C12B	108 ± 19	104.9	n/a
1a	CYP site 1	C19-C12-C22	105 ± 8	104.2	n/a
	CYP site 2	C9-C8-C26	112 ± 11	110.4	n/a
1b	CYP site 1[a]	C9B-C2B-C41[a]	98 ± 12	103.3	n/a
		C9B-C2B-C42[a]	108 ± 12	n/a	n/a
	CYP site 2[a]	C9A-C2A-C11[a]	107 ± 33	105.4	103.5
		C9A-C2A-C12[a]	98 ± 16	102.5	
1c	CYP site 1	C9A-C2A-C12A	110 ± 11	110.9	n/a
	CYP site 2[a]	C9B-C2B-C12D[a]	113 ± 7	110.8	106.9
		C9B-C2B-C12B[a]	101 ± 6	102.9	
1d	CYP site 1	C9A-C2A-C12A	108 ± 7	107.2	n/a
	CYP site 2	C9B-C2B-C12B	107 ± 9	106.6	n/a
1e	CYP site 1	C2-C1-C11	105 ± 8	105.6	n/a

[a] Site is crystallographically disordered.

Table S39. Bending angle of the cyclopropyl-ethynyl axis (θ_{bend}), as shown on Figure 1 of the main text, measured in the experimental crystal structure and DFT-optimized structure. The probe atoms defining the bending angles are given. The experimental errors were estimated using the thermal ellipsoids.

sample	site	probe atoms	experimental θ_{bend} (°)	DFT-optimized θ_{bend} (°)	Transition state θ_{bend} (°)
1	CYP site 1[a]	C2C-C10C-C16A[a]	164 ± 14	175.1	174.4
		C2C-C10C-C16B[a]	167 ± 26	174.6	
	CYP site 2	C2A-C10A-C12A	176 ± 25	176.2	n/a
	CYP site 3	C2B-C10B-C12B	177 ± 29	174.9	n/a
1a	CYP site 1	C12-C20-C22	175 ± 11	174.6	n/a
	CYP site 2	C8-C10-C26	176 ± 15	176.7	n/a
1b	CYP site 1[a]	C2B-C10B-C41[a]	166 ± 20	169.2	n/a
		C2B-C10B-C42[a]	179 ± 19	n/a	n/a
	CYP site 2[a]	C2A-C10A-C11[a]	176 ± 18	175.7	173.4
		C2A-C10A-C12[a]	164 ± 22	171.8	
1c	CYP site 1	C2A-C10A-C12A	177 ± 12	177.7	n/a
	CYP site 2[a]	C2B-C10D-C12D[a]	173 ± 7	176.3	177.0
		C2B-C10B-C12B[a]	177 ± 11	173.3	
1d	CYP site 1	C2A-C10A-C12A	179 ± 13	179.1	n/a
	CYP site 2	C2B-C10B-C12B	178 ± 11	177.8	n/a
1e	CYP site 1	C1-C4-C11	175 ± 11	171.1	n/a

[a] Site is crystallographically disordered.

ORTEP Plots.

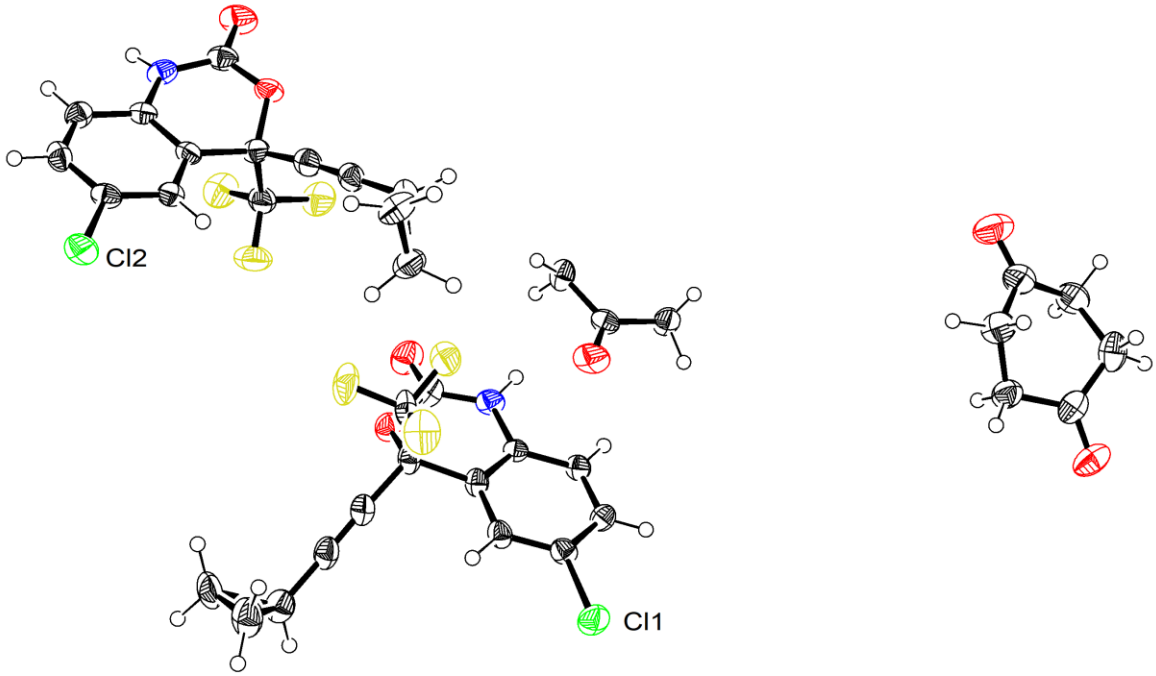

Figure S37. Thermal ellipsoid plot of pure **1a** [(efavirenz)(cyclohexane-1,4-dione)]. This figure was generated using ORTEP-3[10] with structure CSD# 768815 from Mahapatra et al.[6]

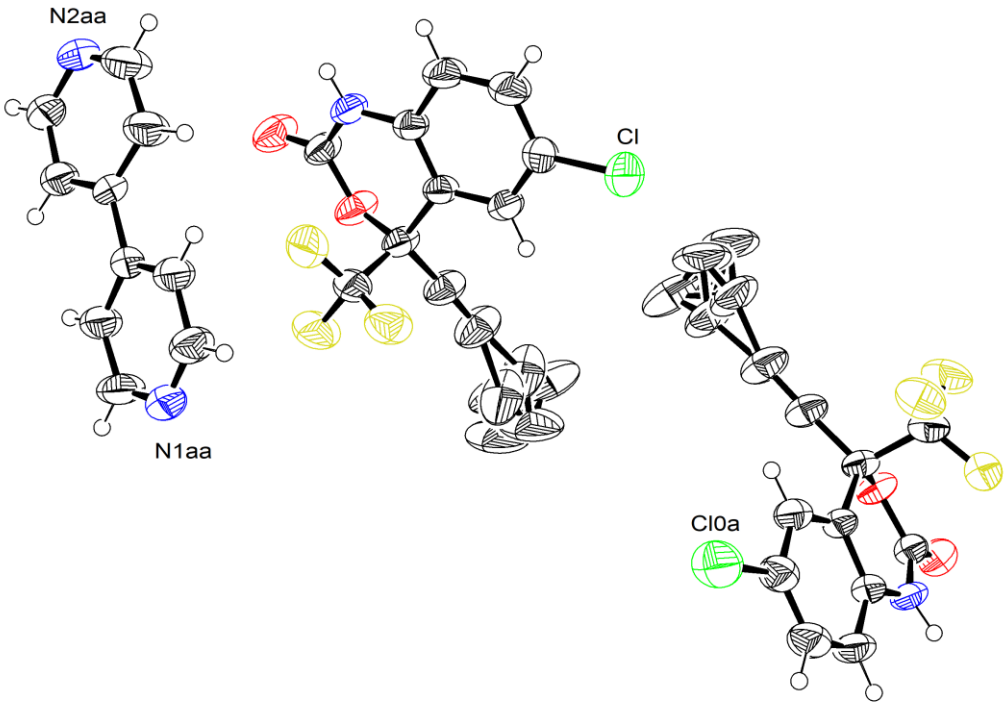

Figure S38. Thermal ellipsoid plot of pure **1b** [(efavirenz)(4,4'-bipyridyl)]. This figure was generated using ORTEP-3[10] with structure CSD# 767759 from Mahapatra et al.[6]

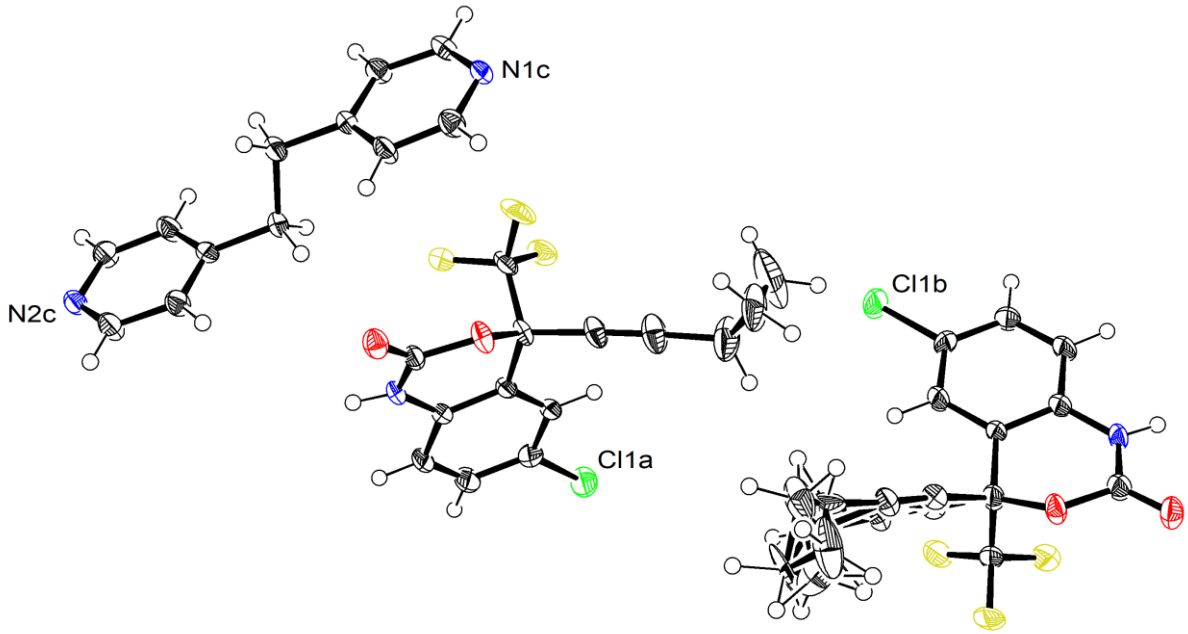

Figure S39. Thermal ellipsoid plot of pure **1c** [(efavirenz)(1,2-di(pyridin-4-yl)ethane)]. This figure was generated using ORTEP-3[10] with structure CSD# 909386 from de Melo et al.[7]

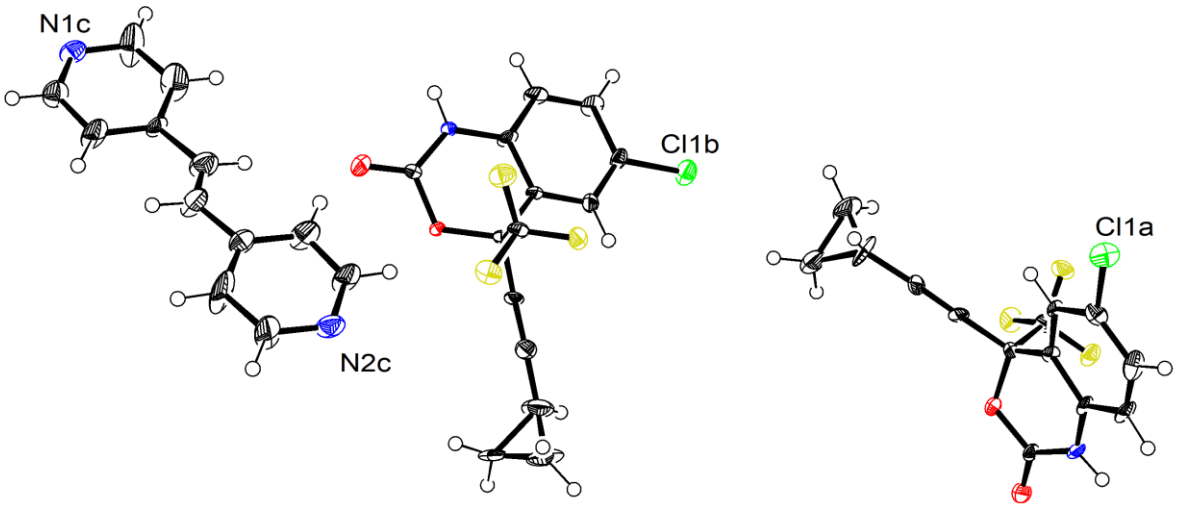

Figure S40. Thermal ellipsoid plot of pure **1d** [(efavirenz)((*E*)-1,2-di(pyridin-4-yl)ethene)]. This figure was generated using ORTEP-3[10] with structure CSD# 909385 from de Melo et al.[7]

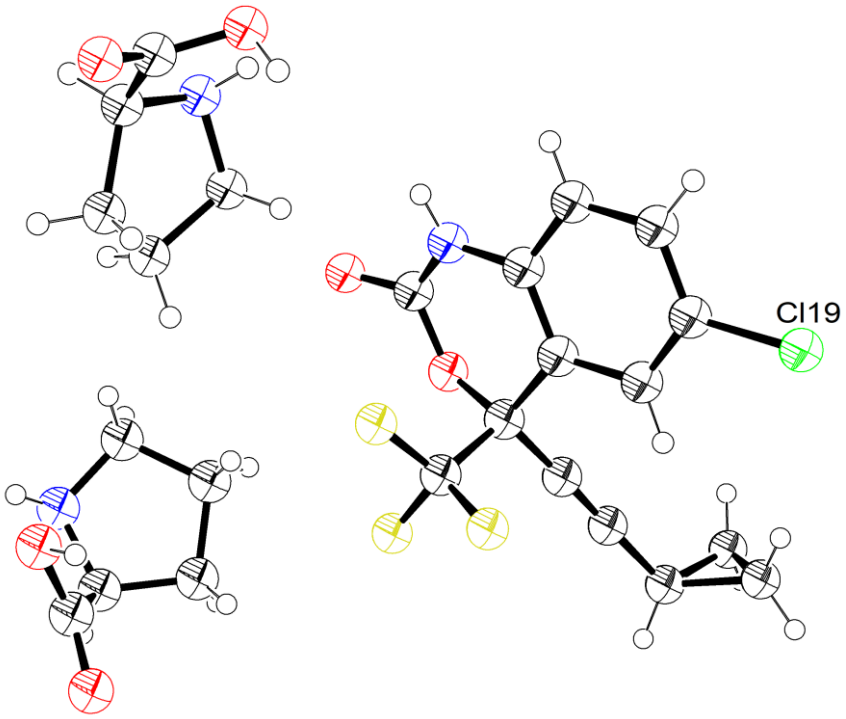

Figure S41. Thermal ellipsoid plot of pure **1e** [(efavirenz)(*L*-proline)]. The thermal ellipsoids are isotropic. This figure was generated using ORTEP-3[10] with structure CSD# 1847168 from Marques et al.[8]

Section V – Crystal Packing.

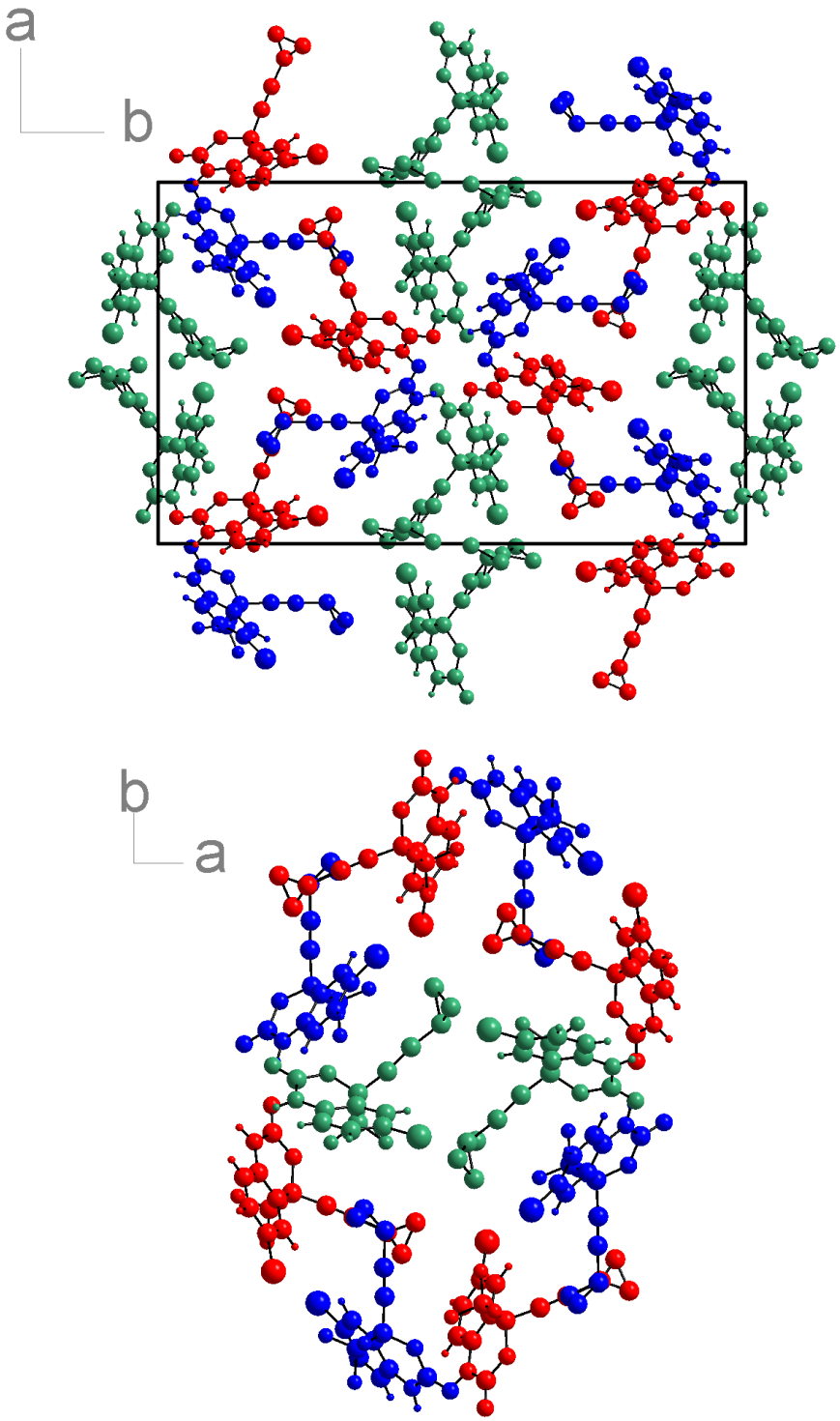

Figure S42. View of the crystallographic packing of **1** along the *c* axis (top) and packing around the disordered Efavirenz molecule (bottom, disorder has been removed). The colouring reflects the three unique molecules in the unit cell, with the disordered efavirenz molecule shown in green, and the black lines denote the unit cell edges. A single cyclopropyl position is shown in the lower figure for clarity. Additional descriptions of the structure can be found in *Cryst. Growth Des.*, 2010, **10**, 3191-3202.[6]

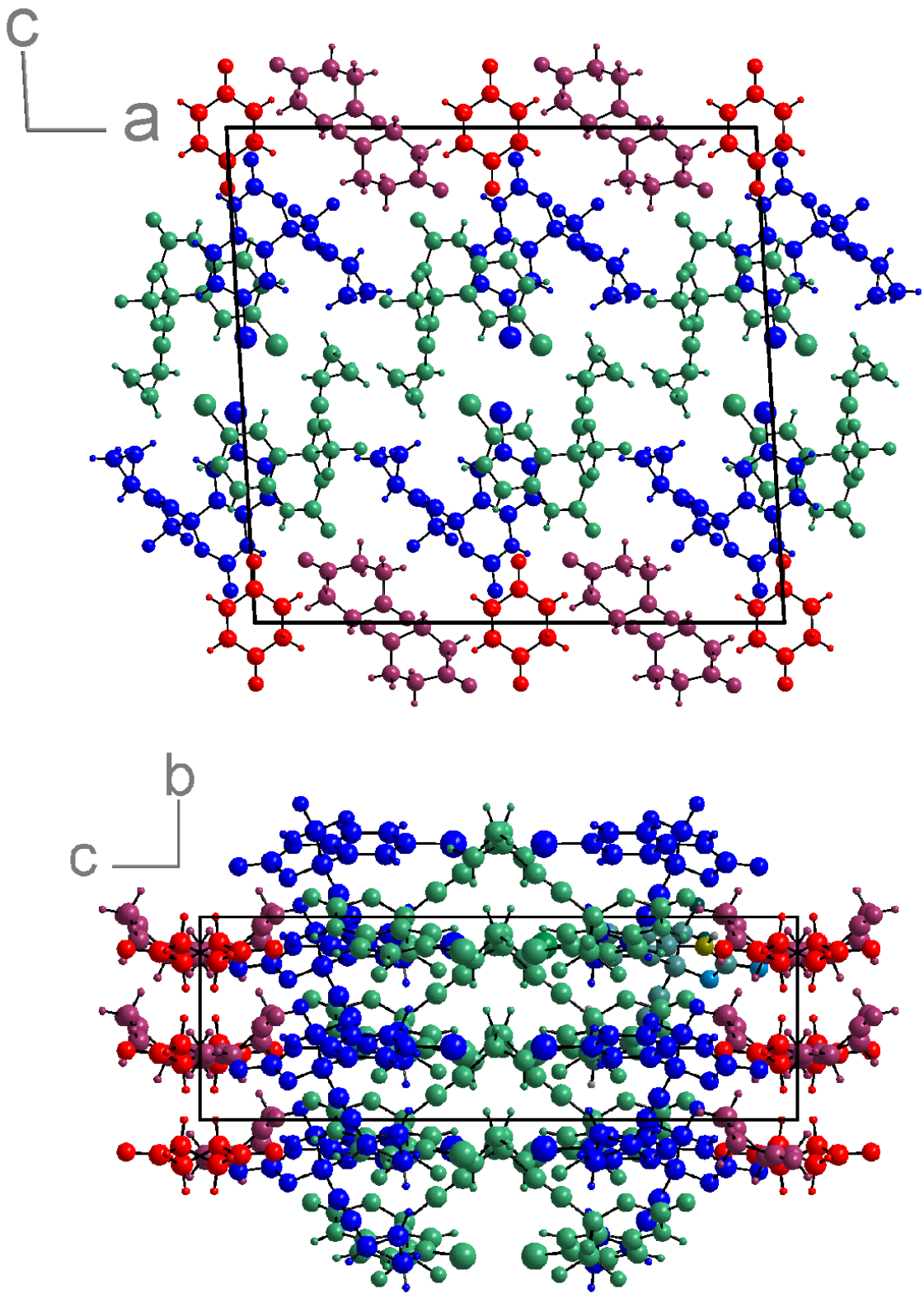

Figure S43. View of the crystallographic packing of **1a** along the *b* axis (top) and the *a* axis (bottom). The colouring reflects the four unique molecules in the unit cell, with the efavirenz molecules shown in green and blue, whereas the cyclohexane-1,4-dione molecules are shown in red and purple. The black lines denote the unit cell edges.

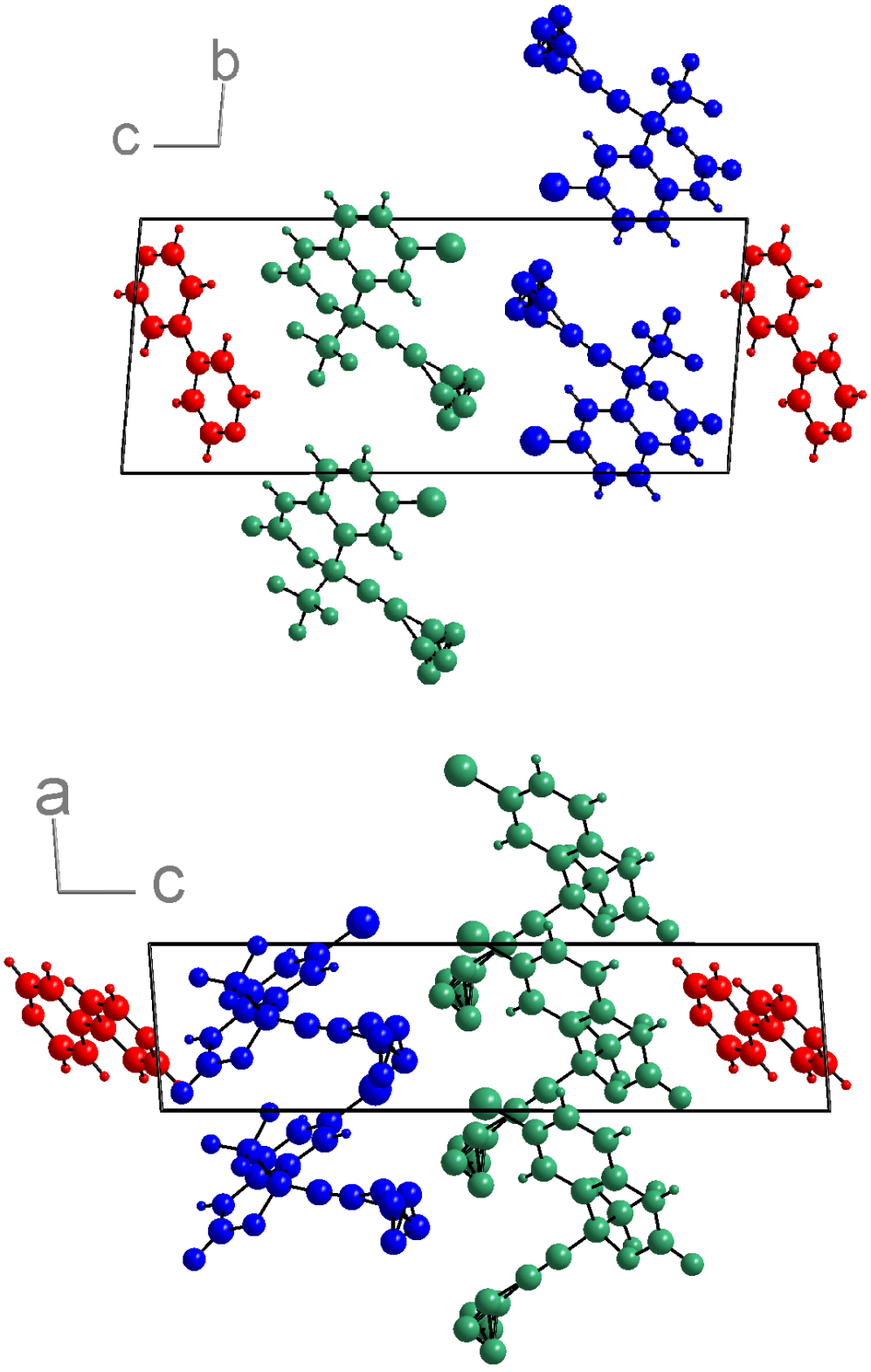

Figure S44. View of the crystallographic packing of **1b** along the *a* axis (top) and the *b* axis (bottom). The colouring reflects the three unique molecules in the unit cell, with the efavirenz molecules shown in green and blue, whereas the 4,4'-bipyridyl molecule is shown in red. The black lines denote the unit cell edges.

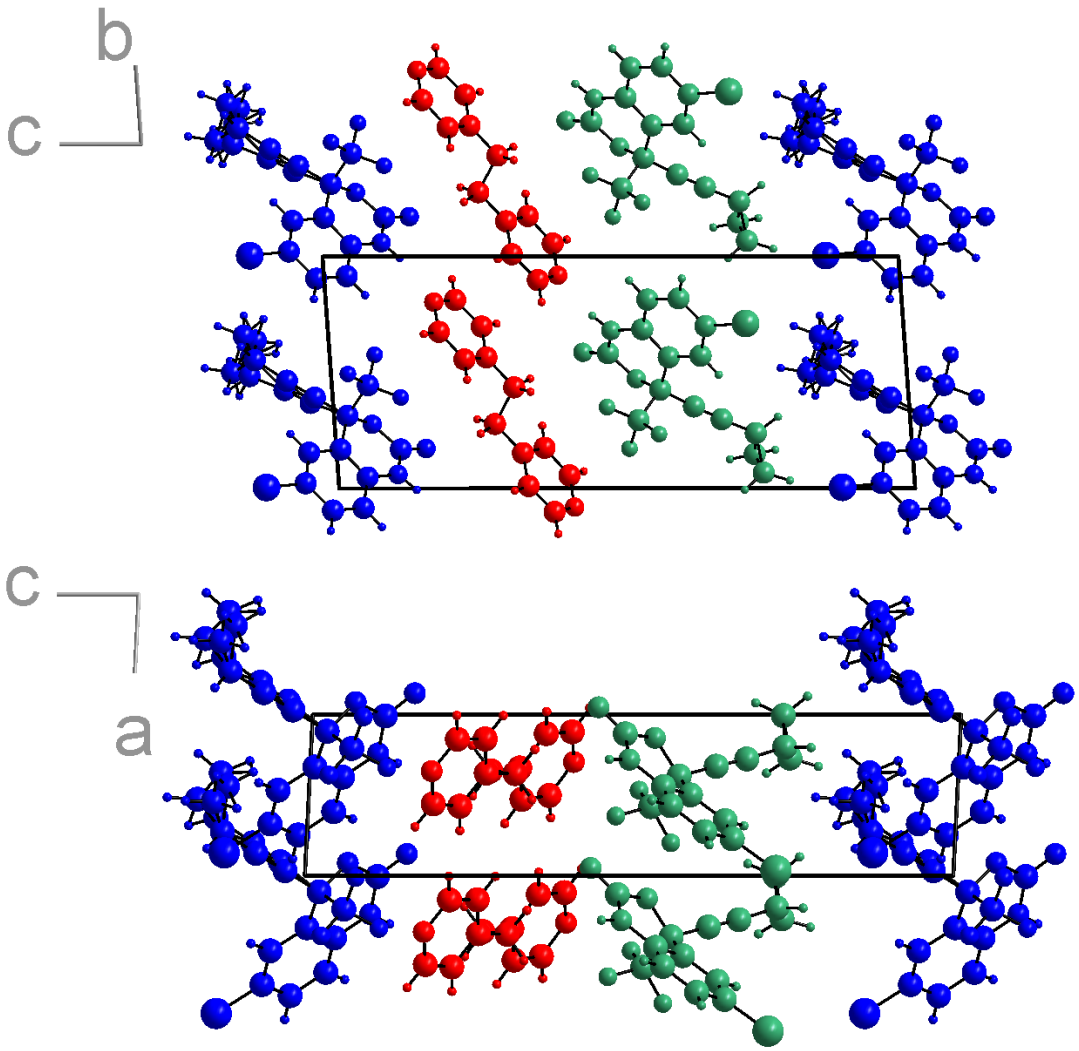

Figure S45. View of the crystallographic packing of **1c** along the *a* axis (top) and the *b* axis (bottom). The colouring reflects the three unique molecules in the unit cell, with the efavirenz molecules shown in green and blue, whereas the 1,2-di(pyridin-4-yl)ethane molecule is shown in red. The black lines denote the unit cell edges.

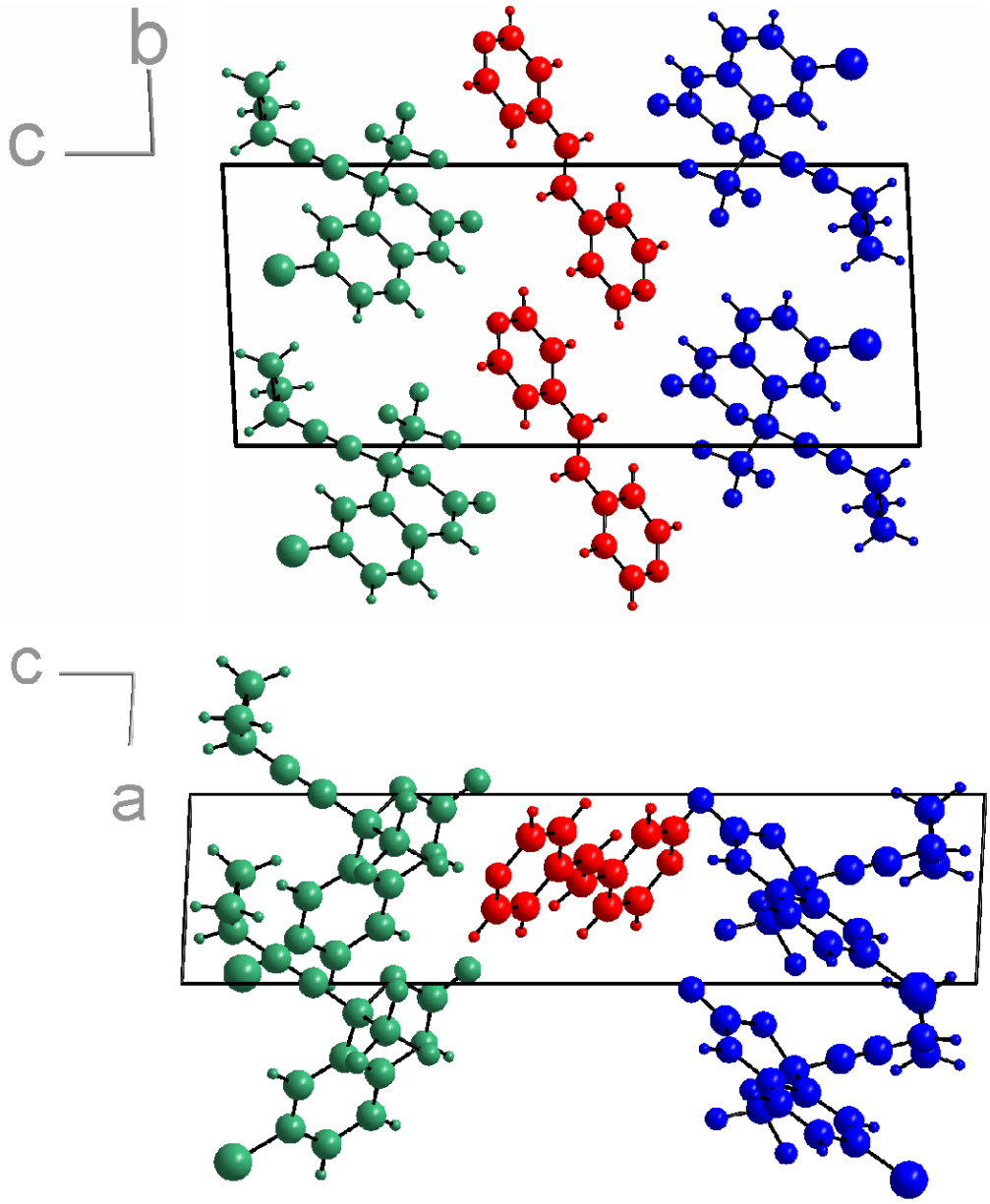

Figure S46. View of the crystallographic packing of **1d** along the *a* axis (top) and the *b* axis (bottom). The colouring reflects the three unique molecules in the unit cell, with the efavirenz molecules shown in green and blue, whereas the (*E*)-1,2-di(pyridin-4-yl)ethene molecule is shown in red. The black lines denote the unit cell edges.

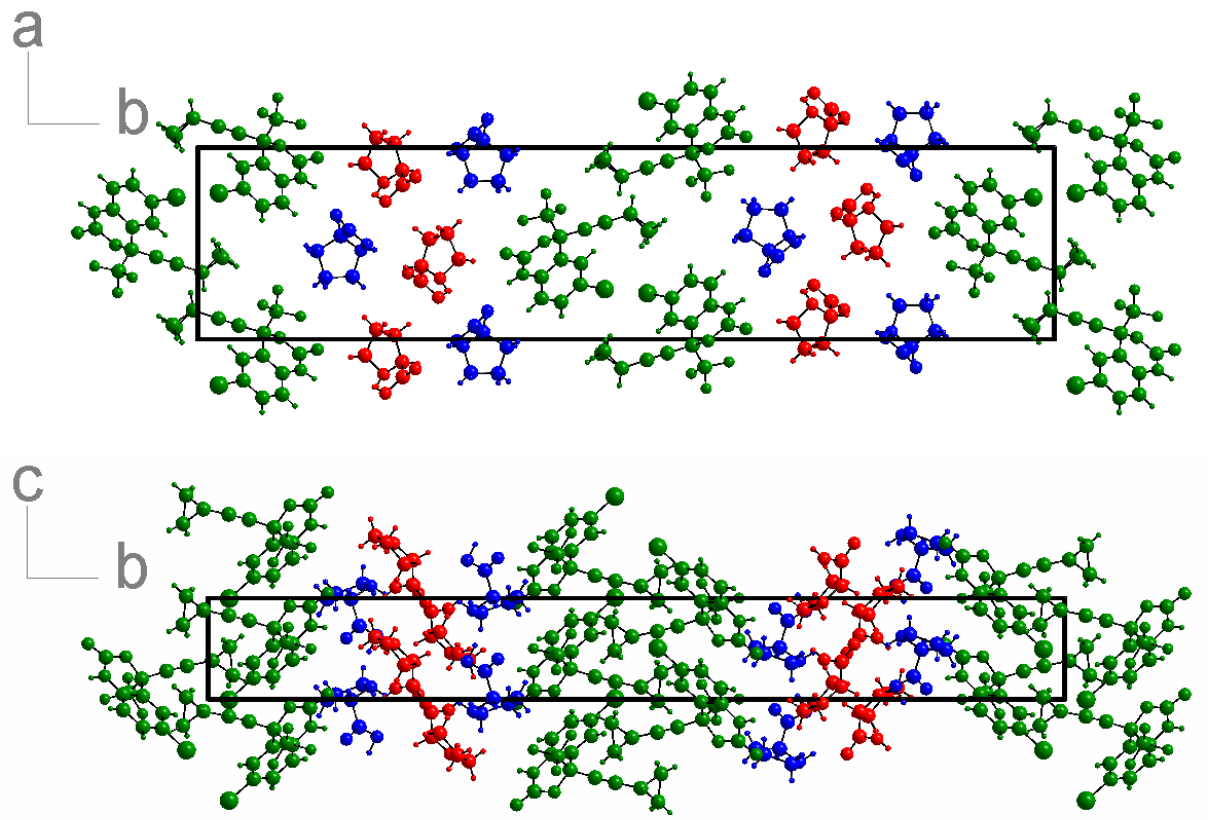

Figure S47. View of the crystallographic packing of **1e** along the *c* axis (top) and *a* axis (bottom). The colouring reflects the three unique molecules in the unit cell, with the efavirenz molecule shown in green and the *L*-proline molecules shown in red and blue. The black lines denote the unit cell edges.

Section VI – Cambridge Structural Database analysis.

Procedure. The Cambridge Structural Database (CSD) version 5.41 update 3 (August 2020) was searched using ConQuest, defining a protonated cyclopropyl group as the search query. The search was repeated, selecting for disordered structures. The results were then manually analysed to identify the cases where disorder is occurring in the cyclopropyl group. Of the 894 results structures with cyclopropyl groups, 166 were disordered, of which 62 featured disorder in the cyclopropyl group. The REFCODE of these structures can be found in Table S40.

Table S40. List of structures on the Cambridge Structural Database (CSD) featuring disorder in the cyclopropyl group.

AJEYAQ	GADKIG	NINQOS	SIWPET
AJEYAQ02	GAPXIG	NUMVOJ	SOZMIG
AJEYAQ04	GIRYIS	OZAVAO	TELGID
BAKROV	HEHHAG	OZICUW	UMESIO
BAKRUB	HIJHUG	PAGWAY	UNOXOM
BERYAZ01	HIJJES	PAKXUX	WOHPUH
BOCMAI	HINGOD	PIVQIU	XATROZ
BOCYAV	HOGNOJ	QUSQOL	XEFGEX
BOKPIB	HUFXIP	ROKNUB	XICRUY
BOZSAN	ICEVUI	ROKNUB02	YEFJUP
CETQAW	IQICOC	RUMLIW	YEFKAW
DUBREZ	KEWPOU	RUTGIW	ZIFRAK
DUBRID	MIJXUA	SALSUW	ZIJFUV
ETOMOR	MIRDEZ	SEGRUS	ZOZYES
FAHSAL	MOVYEC	SIBZIP	
FEXDET	NEHGIT	SIDPAX	

References.

1 Bloch, F. Generalized Theory of Relaxation. *Phys. Rev.* **105**, 1206-1222 (1957).

2 Bloch, F. Dynamical Theory of Nuclear Induction. II. *Phys. Rev.* **102**, 104-135 (1956).

3 Wangsness, R. K. & Bloch, F. The Dynamical Theory of Nuclear Induction. *Phys. Rev.* **89**, 728-739 (1953).

4 Redfield, A. G. On the theory of relaxation processes. *IBM J. Res. Dev.* **1**, 19-31 (1957).

5 Schanda, P. & Ernst, M. Studying Dynamics by Magic-Angle Spinning Solid-State NMR Spectroscopy: Principles and Applications to Biomolecules. *Prog. Nucl. Magn. Reson. Spectrosc.* **96**, 1-46 (2016).

6 Mahapatra, S., Thakur, T. S., Joseph, S., Varughese, S. & Desiraju, G. R. New Solid State Forms of the Anti-HIV Drug Efavirenz. Conformational Flexibility and High Z' Issues. *Cryst. Growth Des.* **10**, 3191-3202 (2010).

7 de Melo, A. C. C., de Amorim, I. F., Cirqueira, M. d. L. & Martins, F. T. Toward Novel Solid-State Forms of the Anti-HIV Drug Efavirenz: From Low Screening Success to Cocrystals Engineering Strategies and Discovery of a New Polymorph. *Cryst. Growth Des.* **13**, 1558-1569 (2013).

8 Marques, M. *et al.* CCDC 1847168: Experimental Crystal Structure Determination. *CSD Communication* (2019)).
9 Pawlak, T. *et al.* Synergy of Solid-State NMR, Single-Crystal X-ray Diffraction, and Crystal Structure Prediction Methods: A Case Study of Teriflunomide (TFM). *Cryst. Growth Des.* **21**, 3328-3343 (2021).
10 Farrugia, L. J. WinGX and ORTEP for Windows: an update. *J. Appl. Crystallogr.* **45**, 849-854 (2012).